

This discussion paper is/has been under review for the journal Atmospheric Chemistry and Physics (ACP). Please refer to the corresponding final paper in ACP if available.

Summertime nitrate aerosol in the upper troposphere and lower stratosphere over the Tibetan Plateau and the South Asian summer monsoon region

Y. Gu^{1,2} and H. Liao¹

¹State Key Laboratory of Atmospheric Boundary Layer Physics and Atmospheric Chemistry (LAPC), Institute of Atmospheric Physics, Chinese Academy of Sciences, Beijing, China

²University of Chinese Academy of Sciences, Beijing, China

Received: 8 October 2015 – Accepted: 5 November 2015 – Published: 13 November 2015

Correspondence to: H. Liao (hongliao@mail.iap.ac.cn)

Published by Copernicus Publications on behalf of the European Geosciences Union.

ACPD

15, 32049–32099, 2015

Summertime nitrate
in the upper
troposphere and
lower stratosphere

Y. Gu and H. Liao

Title Page	
Abstract	Introduction
Conclusions	References
Tables	Figures
 	 
Back	Close
Full Screen / Esc	
Printer-friendly Version	
Interactive Discussion	

Abstract

We use the global three-dimensional Goddard Earth Observing System chemical transport model (GEOS-Chem) to examine the contribution of nitrate aerosol to aerosol concentrations in the upper troposphere and lower stratosphere (UTLS) over the Tibetan Plateau and the South Asian summer monsoon (TP/SASM) region during summertime of year 2005. Simulated surface-layer aerosol concentrations are compared with ground-based observations, and simulated aerosols in the UTLS are evaluated by using the Stratospheric Aerosol and Gas Experiment II satellite data. Simulations show elevated aerosol concentrations of sulfate, nitrate, ammonium, black carbon, organic carbon, and $\text{PM}_{2.5}$ (particles with diameter equal or less than $2.5\text{ }\mu\text{m}$) in the UTLS over the TP/SASM region throughout the summer. Nitrate aerosol is simulated to be the second largest aerosol species in the surface-layer but the most dominant aerosol species in the UTLS over the studied region. Averaged over summertime and over the TP/SASM region, C_{NIT} (the ratio of nitrate concentration to $\text{PM}_{2.5}$ concentration) values are 5–35 % at the surface, 25–50 % at 200 hPa, and exceed 60 % at 100 hPa. The mechanisms for the accumulation of nitrate in the UTLS over the TP/SASM region include vertical transport and the gas-to-aerosol conversion of HNO_3 to form nitrate. The high relative humidity and low temperature associated with the deep convection over the TP/SASM region are favorable for the gas-to-aerosol conversion of HNO_3 .

20 1 Introduction

Aerosols in the upper troposphere and lower stratosphere (UTLS) have much longer residence time than those in the lower troposphere, which influence atmospheric chemistry and the Earth's climate with large spatial and temporal coverage (Rasch et al., 2008). Aerosols in the UTLS influence the concentrations of chemical species via changes in photolysis rates and heterogeneous reactions (Pitari et al., 2014). For example, heterogeneous reactions on sulfate aerosol can perturb the chemical parti-

Summertime nitrate in the upper troposphere and lower stratosphere

Y. Gu and H. Liao

[Title Page](#)

[Abstract](#)

[Introduction](#)

[Conclusions](#)

[References](#)

[Tables](#)

[Figures](#)

◀

▶

[Back](#)

[Close](#)

[Full Screen / Esc](#)

[Printer-friendly Version](#)

[Interactive Discussion](#)



tioning in the lower stratosphere, leading to significant O₃ depletion through enhanced chlorine, bromine, and odd-hydrogen catalytic cycle (Zhao et al., 1997; Considine et al., 2001; Talukdar et al., 2012; Tang et al., 2014; Pitari et al., 2014). Aerosols in the UTLS also influence climate by altering properties of cirrus clouds via homogeneous or heterogeneous ice nucleation (Li et al., 2005; Liu et al., 2009; Yin et al., 2012; Fadnavis et al., 2013). Injection of aerosols into the UTLS has been reported to induce complex responses in circulation, temperature, and water vapor (Liu et al., 2009; Wu et al., 2011; Su et al., 2011; Fadnavis et al., 2013).

Aerosols over the Tibetan Plateau (TP) and the Asian summer monsoon region are especially important. The TP is surrounded by countries with large anthropogenic emissions (Li et al., 2005; Lau et al., 2006). Aerosols from India, Southeast Asia, and southern China can be transported to the TP by prevailing winds in the premonsoon and monsoon seasons (Lawrence and Lelieveld, 2010; Xia et al., 2011). Observational and modeling studies have shown that persistent maxima of atmospheric constituents, such as water vapor (Gettelman et al., 2004; Randel and Park, 2006; Park et al., 2007), CO (Kar et al., 2004; Li et al., 2005; Park et al., 2007, 2008, 2009), CH₄ (M. Park et al., 2004; Xiong et al., 2009), NO_x (M. Park et al., 2004), HCN (Park et al., 2008; Randel et al., 2010), C₂H₆ and C₂H₂ (Park et al., 2008), exist in the UTLS above the TP and the South Asian summer monsoon (SASM) region because of the deep convection during boreal summer. Satellite observations suggested that the convection associated with the SASM is a vital pathway to transport air mass from the lower troposphere into the stratosphere (Chen et al., 2006; Randel and Park, 2006; Randel et al., 2010; Bian et al., 2011a). The heating associated with the persistent deep convection during summertime leads to the formation of the Tibetan anticyclone in the UTLS, which acts to isolate air within the anticyclone and traps the uplifted pollutants at that altitude (Park et al., 2007; Vernier et al., 2011; Bourgeois et al., 2012; Fadnavis et al., 2013; He et al., 2014). The stratosphere–troposphere exchange (STE) over the TP contributes largely to the global STE (Chen et al., 2006).

[Title Page](#)

[Abstract](#)

[Introduction](#)

[Conclusions](#)

[References](#)

[Tables](#)

[Figures](#)

[◀](#)

[▶](#)

[Back](#)

[Close](#)

[Full Screen / Esc](#)

[Printer-friendly Version](#)

[Interactive Discussion](#)



- Previous studies have reported that aerosols exist in the UTLS over the TP/SASM region. Kim et al. (2003) carried out optical measurements with a ground-based lidar in Lhasa from August to October of 1999, and found an enhancement in aerosol concentration near the local tropopause with scattering ratio (SR, the ratio of aerosol plus molecular backscatter to molecular backscatter alone) of 1.1–1.2. Tobo et al. (2007) reported an enhancement of sub-micron aerosols (effective radius $r = 0.15\text{--}0.6\,\mu\text{m}$) near the summertime tropopause (about 130 to 70 hPa), on the basis of in situ balloon measurements from an Optical Particle Counter at the same location in August of 1999. Vernier et al. (2009) examined satellite measurements from the Cloud-Aerosol Lidar with Orthogonal Polarization (CALIOP) onboard Cloud-Aerosol Lidar and Infrared Pathfinder Satellite Observation (CALIPSO) and reported the presence of small depolarizing particles with high SR values (about 1.20 at 532 nm) at 16–17 km altitude over South Asia in July and August of 2007 and 2008. Bourgeois et al. (2012) found that an aerosol layer existed at 16–18 km altitude over the Asian continent and Indian Ocean ($20^\circ\text{ S}\text{--}30^\circ\text{ N}$, $5\text{--}105^\circ\text{ E}$) on the basis of the CALIOP observations. Recently, He et al. (2014) examined the vertical profiles of aerosol extinction coefficients measured with a Micro Pulse Lidar at Naqu, a meteorological station located in the central part of the TP, and also showed a maximum in aerosol extinction coefficient ($\sim 2.10^{-3}\,\text{km}^{-1}$) in the UTLS (18–19 km) during the summer of 2011.
- A number of previous studies have attempted to understand the chemical composition of aerosols in the UTLS. Froyd et al. (2009) measured aerosol composition with the National Oceanic and Atmospheric Administration (NOAA) single-particle mass spectrometer aboard the National Aeronautics and Space Administration (NASA) WB-57 high altitude aircraft platform, and reported that particles in the tropical tropopause layer were rich in nitrogen. Vernier et al. (2011) suggested that aerosol layer at the tropopause of Asia could be sulfur and/or organics, considering that Asian pollutants consisted of black carbon, organic carbon, SO_2 , and NO_x (Park et al., 2009; Randel et al., 2010). Weigel et al. (2011) analyzed the volatility of aerosols obtained from in situ airborne measurements and reported that about 75–90 % of the particles in the tropical

[Title Page](#)[Abstract](#)[Introduction](#)[Conclusions](#)[References](#)[Tables](#)[Figures](#)[◀](#)[▶](#)[Back](#)[Close](#)[Full Screen / Esc](#)[Printer-friendly Version](#)[Interactive Discussion](#)

tropopause layer were volatile (> 75 %), but this study did not give any detailed analyses of chemical composition of aerosols. Bourgeois et al. (2012) showed, by using the ECHAM5.5-HAM2 model, that sulfate, water, and OC contributed, respectively, 53, 29, and 11 % to aerosol extinction in the vicinity of the tropical tropopause layer. The ECHAM5.5-HAM2 model used by Bourgeois et al. (2012) simulated all major aerosol species in the atmosphere except for nitrate.

Few previous studies have examined nitrate aerosol in the UTLS, although nitrate is expected to be important for the following reasons. First, emissions of precursors of nitrate, such as NO_x and NH_3 , are high over India, Southeast Asia, and China (Streets et al., 2003; Datta et al., 2012; Huang et al., 2012). Second, simulated nitrate concentrations are high over those regions (Liao and Seinfeld, 2005; Mu and Liao, 2014; Lou et al., 2014). Third, measured concentrations of nitrate are comparable to or larger than those of sulfate at rural and urban sites in the SASM region. Shrestha et al. (2000) carried out measurements of aerosols at Phortse, Nepal, during September 1996–November 1997, and showed that the average concentration of nitrate during the monsoon season (June–September) was $0.34 \mu\text{g m}^{-3}$, higher than that of sulfate ($0.17 \mu\text{g m}^{-3}$). Decesari et al. (2010) reported, on the basis of measurements at the Nepal Climate Observatory-Pyramid from 2006 to 2008, that the concentrations of nitrate and sulfate were 0.37 and $0.50 \mu\text{g m}^{-3}$, respectively, during the monsoon season. Chatterjee et al. (2010) measured aerosols at a high altitude station in northeastern Himalayas during January–December 2005. They found that the average concentrations of fine-mode nitrate and sulfate were $3.31 \pm 2.25 \mu\text{g m}^{-3}$ and $3.80 \pm 2.9 \mu\text{g m}^{-3}$, respectively. At Lahore, an urban site in Pakistan, the observed daytime nitrate concentration of $21.8 \mu\text{g m}^{-3}$ was also higher than sulfate concentration of $12.6 \mu\text{g m}^{-3}$ (Lodhi et al., 2009), as the observations were averaged over November 2005 to March 2006. Fourth, the low temperatures in the UTLS would favor nitrate formation (Seinfeld and Pandis, 2006). Therefore, it is of interest to take nitrate aerosol into consideration when we examine aerosols in the UTLS.

[Title Page](#)

[Abstract](#)

[Introduction](#)

[Conclusions](#)

[References](#)

[Tables](#)

[Figures](#)

◀

▶

[Back](#)

[Close](#)

[Full Screen / Esc](#)

[Printer-friendly Version](#)

[Interactive Discussion](#)



In this work we simulate nitrate aerosol and its contribution to aerosol concentrations in the UTLS over the TP ($70\text{--}105^\circ\text{ E}$, $25\text{--}40^\circ\text{ N}$) and the SASM region ($70\text{--}105^\circ\text{ E}$, $10\text{--}25^\circ\text{ N}$) by using the global chemical transport model GEOS-Chem driven by the assimilated meteorological fields. These regions of interest are shown in Fig. 1. Simulated surface-layer aerosol concentrations are compared with ground-based observations, and simulated aerosols in the UTLS are evaluated by using the Stratospheric Aerosol and Gas Experiment II (SAGE II) satellite data. Section 2 is a brief description of the GEOS-Chem model and numerical experiment. Section 3 presents the simulation and evaluation of distributions and concentrations of HNO_3 and O_3 to show model's capability in simulating the $\text{NO}_x\text{-O}_3\text{-HNO}_3$ cycle over the studied regions. Section 4 shows simulated aerosols and Sect. 5 presents the simulated contribution of nitrate to aerosol concentrations in the UTLS over the TP and the SASM region. Section 6 discusses the mechanisms for high concentrations of nitrate in the UTLS.

2 Model description and numerical experiment

15 2.1 GEOS-Chem model

We simulate gas-phase species and aerosols using the global chemical transport model GEOS-Chem (version 9-01-03, <http://acmg.seas.harvard.edu/geos/index.html>) driven by the GEOS-5 assimilated meteorological fields from the Goddard Earth Observing System of the NASA Global Modeling and Assimilation Office. The version of the model used here has a horizontal resolution of 2° latitude by 2.5° longitude and 20 vertical layers extending from the surface to 0.01 hPa. Over the TP and the SASM region, the model has about 34 layers in the troposphere and 12 layers in the stratosphere.

The GEOS-Chem model has a fully coupled treatment of tropospheric $\text{NO}_x\text{-CO}$ -hydrocarbon-aerosol chemistry and aerosols including sulfate (SO_4^{2-}), nitrate (NO_3^-), ammonium (NH_4^+), organic carbon (OC), black carbon (BC) (R. J. Park et al., 2003,

[Title Page](#)[Abstract](#)[Introduction](#)[Conclusions](#)[References](#)[Tables](#)[Figures](#)[◀](#)[▶](#)[Back](#)[Close](#)[Full Screen / Esc](#)[Printer-friendly Version](#)[Interactive Discussion](#)

2004; Pye et al., 2009), mineral dust (Fairlie et al., 2007), and sea salt (Alexander et al., 2005; Jaeglé et al., 2011). The gas-aerosol partitioning of nitric acid and ammonium is calculated using the ISORROPIA II thermodynamic equilibrium model (Fountoukis and Nenes, 2007). The two-way coupling between aerosols and gas phase chemistry provides consistent chemical fields for aerosol simulation and aerosol mass for heterogeneous processes and calculations of gas-phase photolysis rates. Heterogeneous reactions include hydrolysis of N_2O_5 (Evans and Jacob, 2005), irreversible absorption of NO_3^- and NO_2 on wet aerosols (Jacob, 2000), and the uptake of HO_2 by aerosols (Liao and Seinfeld, 2005; Thornton et al., 2008).

With respect to chemistry in the stratosphere, stratospheric O_3 concentrations are calculated using the linearized parameterization scheme (McLinden et al., 2000). The monthly mean production rates and loss frequencies of species other than O_3 use those from NASA Global Modeling Initiative (GMI) Combo simulations using MERRA met fields (Duncan et al., 2007; Considine et al., 2008; Murray et al., 2012).

Convective transport in GEOS-Chem mimics that in the parent GEOS general circulation model (GCM) (Hack, 1994; Zhang and McFarlane, 1995), which accounts for updraft, downdraft, and entrainment mass fluxes for deep and shallow convection (Wu et al., 2007). The aerosol wet deposition scheme in the GEOS-Chem follows that of Liu et al. (2001). For the scavenging of aerosols, SO_4^{2-} , NO_3^- , NH_4^+ , and hydrophilic OC and BC aerosols are assumed to be fully soluble. Dry deposition follows the standard resistance-in-series model of Wesely (1989).

Global emissions of aerosols and their precursors in the GEOS-Chem follow R. J. Park et al. (2003, 2004), with anthropogenic emissions of NO_x , CO, SO_2 , and non-methane volatile organic compounds (NMVOC) in Asia overwritten by David Streets' 2006 emission inventory (<http://mic.greenresource.cn/intex-b2006>). Emissions of NH_3 in Asia are taken from Streets et al. (2003). Since NH_3 emissions in China showed large uncertainties in previous studies (Streets et al., 2003; Kim et al., 2006; Y. Zhang et al., 2010; Huang et al., 2011, 2012), we use the most recent estimate of NH_3 emissions in China by Huang et al. (2012), which is 9.8 Tg yr^{-1} , instead of 13.5 Tg yr^{-1} from

Summertime nitrate in the upper troposphere and lower stratosphere

Y. Gu and H. Liao

[Title Page](#)

[Abstract](#)

[Introduction](#)

[Conclusions](#)

[References](#)

[Tables](#)

[Figures](#)

◀

▶

[Back](#)

[Close](#)

[Full Screen / Esc](#)

[Printer-friendly Version](#)

[Interactive Discussion](#)



Summertime nitrate in the upper troposphere and lower stratosphere

Y. Gu and H. Liao

[Title Page](#)

[Abstract](#)

[Introduction](#)

[Conclusions](#)

[References](#)

[Tables](#)

[Figures](#)

◀

▶

[Back](#)

[Close](#)

[Full Screen / Esc](#)

[Printer-friendly Version](#)

[Interactive Discussion](#)



3 Simulated concentrations of HNO₃ and O₃ and model evaluation

Nitrate aerosol forms when nitric acid (HNO₃) reacts with alkaline gases (for example, ammonia) in the atmosphere (Seinfeld and Pandis, 2006). HNO₃, as the important precursor of nitrate, is the major oxidation product of nitrogen oxides (NO_x = NO + NO₂)

5 (Seinfeld and Pandis, 2006). To show the model's capability in simulating the NO_x-O₃-HNO₃ cycle over the studied regions, we present and evaluate the simulated HNO₃ and O₃ in this section.

Simulated mixing ratios of HNO₃ and O₃ in the UTLS are evaluated by using datasets from the limb viewing satellite instrument of Microwave Limb Sounder (MLS, version 4.2, level 2, ftp://acddisc.gsfc.nasa.gov/data/s4pa//Aura MLS_Level2/). The MLS datasets provide valuable information on atmospheric compositions in the UTLS (Walters et al., 2006). For HNO₃, the MLS provides datasets for 316 to 68 hPa, with a vertical resolution of 3–4 km and a horizontal resolution of 400–500 km. Since further evaluations are needed for datasets at altitudes with pressures higher than 215 hPa (Livesey et al., 2015), we use only datasets for pressures lower than that. For O₃, the MLS provides datasets for 261 to 0.02 hPa, with a vertical resolution of 3–3.5 km and a horizontal resolution of 300–350 km in the UTLS (Santee et al., 2007; Livesey et al., 2015). The uncertainties of the MLS HNO₃ and O₃ datasets in the UTLS are about ±0.5–1 ppbv (±5–10 %) and 0.02–0.03 ppmv, respectively (Livesey et al., 2015).

20 3.1 HNO₃

Figure 3a shows the simulated global distribution of HNO₃ concentrations averaged over June–August of 2005. Concentrations of HNO₃ exceed 1 ppbv over the industrialized areas such as Europe, North America, central and eastern Asia, in agreement with the distributions and magnitudes reported in Liao et al. (2003). Over South Asia, simulated HNO₃ concentrations are high (0.3–1 ppbv) in the northern Indian subcontinent, because the emissions of NO_x and NH₃ are high in this region (Streets et al., 2003; Zhang et al., 2009; Datta et al., 2012).

[Title Page](#)

[Abstract](#)

[Introduction](#)

[Conclusions](#)

[References](#)

[Tables](#)

[Figures](#)

◀

▶

[Back](#)

[Close](#)

[Full Screen / Esc](#)

[Printer-friendly Version](#)

[Interactive Discussion](#)



Figure 4a and b shows the simulated HNO_3 concentrations in the UTLS averaged over June–August of 2005. Since the tropopause is located at 70–150 hPa (12–15 km) over the TP/SASM region (Li et al., 2005; Bian et al., 2011b; Fadnavis et al., 2014), we choose the vertical layers of 200 and 100 hPa to represent the UTLS. At both 200 and 100 hPa, the highest HNO_3 concentrations are simulated to occur in the high latitude regions in the Northern Hemisphere (NH) (Fig. 3a and b). Simulated HNO_3 concentrations at 100 hPa are low over the region of 40–100° E and 10–30° N, which is part of the anticyclone region defined in Fig. 1. Figure 4c shows the latitude–altitude cross section of simulated seasonal mean HNO_3 mixing ratios averaged over 70–105° E. In boreal summer, the highest HNO_3 mixing ratios are simulated to occur at 30 hPa over the Polar Regions in both hemispheres. Over high latitudes, HNO_3 concentrations in the Southern Hemisphere (SH) are simulated to be higher than those in the NH.

To evaluate the simulated HNO_3 , Fig. 4d–f shows HNO_3 concentrations in the UTLS from MLS that are averaged over June–August of 2005. At 200 and 100 hPa altitudes, the observed HNO_3 mixing ratios are high in the high latitudes in the NH, which are captured by the GEOS-Chem model. The observed HNO_3 at 100 hPa exhibits low values of less than 240 pptv over 30–100° E and 10–30° N in the Asian monsoon anticyclone region (Fig. 4e). At 100 hPa, the observed HNO_3 mixing ratio averaged over the TP/SASM region (70–105° E, 10–40° N) is 301.3 pptv, which is lower than the simulated values of 345.9 pptv. The difference between the simulated and observed HNO_3 mixing ratio lies within the confidence range of ±500–1000 pptv of the MLS instruments (Livesey et al., 2015). The observed pattern of the HNO_3 vertical distribution (Fig. 4f) is also captured by the GEOS-Chem model (Fig. 4c). The distributions of HNO_3 in the UTLS are associated with the Brewer–Dobson (BD) circulation proposed by Brewer (1949) and Dobson (1956), traveling upwards across the tropopause to the stratosphere at the equator and downwards to the troposphere near the Polar region.

[Title Page](#)[Abstract](#)[Introduction](#)[Conclusions](#)[References](#)[Tables](#)[Figures](#)[◀](#)[▶](#)[◀](#)[▶](#)[Back](#)[Close](#)[Full Screen / Esc](#)[Printer-friendly Version](#)[Interactive Discussion](#)

3.2 O₃

Figure 3b shows the global distribution of simulated summertime surface-layer O₃ concentrations. Simulated O₃ concentrations are in a range of 40–70 ppbv over Europe, North America, China, and the biomass burning region of South Africa. Our model results agree closely with the simulated distributions and magnitudes reported in Mickley et al. (1999), Collins et al. (2000), Liao et al. (2003), Wu et al. (2008), Zeng et al. (2008), and Fadnavis et al. (2014). Fadnavis et al. (2014) also presented aircraft measurements over India in September of 2010 during the Cloud Aerosol Interaction and Precipitation Enhancement Experiment (CAIPEEX). Our simulated O₃ concentrations of 30–40 ppbv over India agree with the CAIPEEX measurements.

Figure 5a and b show the simulated O₃ concentrations in the UTLS averaged over June–August of 2005. The distributions of O₃ concentrations in the UTLS are similar to those of HNO₃, with elevated values in the high latitudes of the NH. Relatively low O₃ mixing ratios of less than 200 ppbv are simulated at 100 hPa over 10–30° N, 20–110° E, within the anticyclone region defined in Fig. 1. Our simulated distributions and magnitudes of O₃ agree with those reported in Bian et al. (2011b), which examined the summertime distributions of O₃ in the UTLS during 2005–2009 by using the MLS version 2.2 level 2 products (Livesey et al., 2008). Because the background O₃ concentrations are generally high in the UTLS and the stratosphere, the low O₃ concentrations in the UTLS over the TP/SASM region are caused by the deep convection that transports O₃-poor air upward (Fu et al., 2006; Randel and Park, 2006; Park et al., 2007; Bian et al., 2011b). Figure 5c displays the latitude-altitude cross section of seasonal mean O₃ mixing ratios averaged over 70–105° E. As a result of the BD circulation, O₃ concentrations in the UTLS are lower over the tropics than in the Polar Regions, even though the maximum O₃ concentrations are located around 10 hPa over the tropics (Brewer, 1949). Our simulated O₃ concentrations in the UTLS agree well with the measurements from MLS (Fig. 5d–f). Our simulated global STE of O₃ is 420 Tgyr⁻¹, which is within the range reported in previous studies (475 ± 120 Tgyr⁻¹ in McLinden

Title Page	
Abstract	Introduction
Conclusions	References
Tables	Figures
	
	
Full Screen / Esc	
Printer-friendly Version	
Interactive Discussion	

et al. (2000), 420 Tg yr^{-1} in Škerlak et al., 2014, $556 \pm 154 \text{ Tg yr}^{-1}$ in Stevenson et al., 2006, and $550 \pm 140 \text{ Tg yr}^{-1}$ in Solomon et al., 2007).

In addition to the comparisons against MLS products, the simulated O_3 profiles are compared with balloon-borne sonde measurements in Fig. 6. The measurements were carried out at Kunming (KM, 102.7°E , 25.0°N) in August of 2009 and at Lhasa (LH, 91.1°E , 29.7°N) in August of 2010. The tropospheric air in LH was less polluted than in KM, and the uncertainties of the observed O_3 mixing ratios were estimated to be within 5–10 % (Bian et al., 2012). In the troposphere, the model underestimates O_3 mixing ratios in KM, while it overestimates O_3 mixing ratios in LH. Since the model results represent the averages over $2^\circ \times 2.5^\circ$ grid cells, the simulated O_3 mixing ratios may not capture well the local variations in emissions. At 100 hPa, the simulated and observed O_3 mixing ratios are, respectively, 112.6 and 124.2 ppbv at KM, and 152.6 and 142.4 ppbv at LH. The magnitudes of O_3 mixing ratios from these balloon-borne sonde measurements support those from MLS; O_3 mixing ratios in the UTLS are less than 200 ppbv over the TP/SASM region.

4 Simulated aerosols and model evaluation

4.1 Simulated aerosols

Figure 7a shows the simulated surface-layer concentrations of SO_4^{2-} , NO_3^- , NH_4^+ , OC, BC, and $\text{PM}_{2.5}$ (the sum of the mass of SO_4^{2-} , NO_3^- , NH_4^+ , BC, and OC aerosols) averaged over June–August of year 2005. As expected, simulated aerosol concentrations are high over polluted regions such as India and eastern China as a result of the high anthropogenic emissions of aerosol precursors and aerosols (Streets et al., 2003; Huang et al., 2012). Over the TP/SASM region ($70\text{--}105^\circ \text{E}$, $10\text{--}40^\circ \text{N}$), the average concentrations of SO_4^{2-} , NO_3^- , NH_4^+ , BC, and OC are 1.69, 0.94, 0.85, 0.30, and $0.94 \mu\text{g m}^{-3}$, respectively. NO_3^- is simulated to be the second largest aerosol species

[Title Page](#)[Abstract](#)[Introduction](#)[Conclusions](#)[References](#)[Tables](#)[Figures](#)[◀](#)[▶](#)[Back](#)[Close](#)[Full Screen / Esc](#)[Printer-friendly Version](#)[Interactive Discussion](#)

**Summertime nitrate
in the upper
troposphere and
lower stratosphere**

Y. Gu and H. Liao

[Title Page](#)[Abstract](#)[Introduction](#)[Conclusions](#)[References](#)[Tables](#)[Figures](#)[◀](#)[▶](#)[◀](#)
[Back](#)[▶](#)
[Close](#)[Full Screen / Esc](#)[Printer-friendly Version](#)[Interactive Discussion](#)

over the region of our interest. The simulated distributions and magnitudes of these aerosol species are similar to those reported in Wang et al. (2013) and Mu and Liao (2014).

Figure 7b and c also show the simulated concentrations of SO_4^{2-} , NO_3^- , NH_4^+ , OC, BC, and $\text{PM}_{2.5}$ in the UTLS. Elevated concentrations of SO_4^{2-} , NO_3^- , NH_4^+ , OC, BC and $\text{PM}_{2.5}$ are simulated over the TP and Plateau south slope at 200 hPa altitude, and extend from eastern Mediterranean to western China at 100 hPa. The simulated enhanced concentrations of SO_4^{2-} , OC, and BC at 100 hPa over the anticyclone region ($20\text{--}120^\circ \text{E}$, $10\text{--}40^\circ \text{N}$) agree with previous observational and modeling studies (Lelieveld et al., 2002; Li et al., 2005; Fadnavis et al., 2013). Li et al. (2005) reported elevated CO concentrations in the upper troposphere over the TP, on the basis of both MLS measurements and the GEOS-Chem simulation for September 2004. Fadnavis et al. (2013) also simulated maximum concentrations of SO_4^{2-} , OC, BC, and mineral dust aerosols in the UTLS during the Asian summer monsoon season owing to convective uplifting of the boundary layer pollutants. With NO_3^- aerosol accounted for in our simulation, NO_3^- is simulated to be the most dominant aerosol species in the UTLS over the TP/SASM region, followed by SO_4^{2-} , NH_4^+ , OC, and BC. At 100 hPa, the averaged concentrations of SO_4^{2-} , NO_3^- , NH_4^+ , OC, and BC over the TP/SASM region ($70\text{--}105^\circ \text{E}$, $10\text{--}40^\circ \text{N}$) region are 0.026, 0.069, 0.014, 0.011, and $0.002 \mu\text{g m}^{-3}$, respectively.

4.2 Comparisons of simulated aerosol concentrations with in-situ observations

The simulated aerosol concentrations in East Asia in the GEOS-Chem model have been evaluated in previous studies (L. Zhang et al., 2010; Fu et al., 2012; Jeong and Park, 2013; Jiang et al., 2013; Wang et al., 2013; Lou et al., 2014). Here we are focused on the evaluation of aerosols in the South Asian monsoon region. For lack of publicly accessible in situ measurements of summertime aerosols in South Asia monsoon area, we compiled monthly or seasonal mean measured concentrations of each



Summertime nitrate in the upper troposphere and lower stratosphere

Y. Gu and H. Liao

Title Page

Abstract

Introduction

Conclusions

References

Tables

Figures

◀

▶

◀
Back

▶
Close

Full Screen / Esc

Printer-friendly Version

Interactive Discussion

aerosol species based on measurements reported in the literature (see Table S1 in the Supplement). These measurements were carried out over years of 1992–2010. The locations of sites with measurements available are shown in Fig. 8a. Most sites are located in the upwind directions of the TP, with pollutants that can be transported to the UTLS during the South Asian summer monsoon season. The observed PM_{10} concentrations listed in Table S1 are multiplied by 0.6 to convert to $\text{PM}_{2.5}$ for model evaluation, following the suggestions in Zhang et al. (2002).

Figure 8b–j shows the scatterplots of simulated vs. observed seasonal mean aerosol concentrations. Compared with measurements, simulated SO_4^{2-} , NO_3^- , NH_4^+ , OC and BC have normalized mean biases (NMB) of -17.0 , $+38.8$, $+42.0$, -69.7 and -41.0% , respectively, as the concentrations of all seasons are considered. The correlations between model results and observations have R values of 0.49 – 0.85 for all aerosol species, indicating that the model is capable of capturing the spatial distributions and seasonal variations of each aerosol species in the South Asian monsoon region despite the biases in concentrations. If we consider simulated and measured concentrations for JJA alone, the simulated concentrations of SO_4^{2-} , NO_3^- , NH_4^+ , OC and BC exhibit seasonal NMB of -15.3 , $+51.5$, $+74.9$, -57.2 and -32.2% , respectively, and the values of R are in the range of 0.24 – 0.85 . Note that the measurements of NO_3^- and NH_4^+ are quite limited in terms of the number of samples, and the discrepancies between model results and measurements may also arise from the mismatch of the model year 2005 with the years of 1992–2010 with observations available.

4.3 Comparisons of simulated aerosol extinction coefficients with SAGE II datasets

Satellite datasets from the Stratospheric Aerosol and Gas Experiment II (SAGE II, <http://sage.nasa.gov/SAGE2/>) are used to evaluate the simulated aerosol extinction in the UTLS. The SAGE II instrument was launched in October 1984 aboard the Earth Radiation Budget Satellite (ERBS) and terminated on 8 September 2005 (McCormick et al., 1987; Chu et al., 1989). The datasets used here are aerosol extinction coeffi-

Summertime nitrate
in the upper
troposphere and
lower stratosphere

Y. Gu and H. Liao

Title Page	
Abstract	Introduction
Conclusions	References
Tables	Figures
 	 
Back	Close
Full Screen / Esc	
Printer-friendly Version	
Interactive Discussion	



Comparisons of profiles of aerosol extinction coefficients with and without nitrate aerosol indicate that the profiles show small differences in altitudes less than 6 km but large discrepancies from 6 km to the tropopause. With nitrate aerosol accounted for, the simulated aerosol extinction coefficients agree closely with SAGE II datasets in the UTLS (averaged over 14–16 km, the simulated value is $8.6 \times 10^{-4} \text{ km}^{-1}$ while the observed value is $8.0 \times 10^{-4} \text{ km}^{-1}$). Without nitrate aerosol, the simulated aerosol extinction coefficient at 14–16 km altitude is $1.5 \times 10^{-4} \text{ km}^{-1}$, which underestimates the aerosol extinction coefficient by 82.6 % compared to that calculated with all the aerosol species. These comparisons of extinction coefficients with and without nitrate aerosol suggest that nitrate aerosol plays an important role in aerosol extinction in the UTLS over the region of our interest.

5 Contribution of nitrate to aerosol concentrations in the UTLS

Since nitrate aerosol is simulated to be the most abundant aerosol species in the UTLS over the TP/SASM region, we analyze the contribution of nitrate to PM_{2.5} concentration ($C_{\text{NIT}} = \text{nitrate concentration}/\text{PM}_{2.5} \text{ concentration}$) in this section. Figure 10 shows the simulated seasonal mean distributions of C_{NIT} for June–August of year 2005. At the surface layer (Fig. 10a), simulated high C_{NIT} values are located over the areas with high nitrate concentrations (India and eastern China) as well as the oceans where NO₃⁻ also forms on sea salt and mineral dust particles (Arimoto et al., 1996; Nakamura et al., 2005; George and Nair, 2008). Over the TP/SASM region, the C_{NIT} values in JJA are 5–35 % at the surface, 25–50 % at 200 hPa (Fig. 10b), and exceed 60 % at 100 hPa (Fig. 10c). The latitude–altitude cross section of C_{NIT} (Fig. 10d) shows that C_{NIT} over 20–40° N increases with altitude and reaches maximum values around the extratropical tropopause.

Table 2 lists the mean concentrations of SO₄²⁻, NO₃⁻, NH₄⁺, BC and OC, and their contributions to PM_{2.5} during summertime of 2005 over the TP/SASM, TP, and SASM regions. Over the TP/SASM region, SO₄²⁻, NO₃⁻, NH₄⁺, BC and OC are simulated to

[Title Page](#)[Abstract](#)[Introduction](#)[Conclusions](#)[References](#)[Tables](#)[Figures](#)[◀](#)[▶](#)[◀](#)[▶](#)[Back](#)[Close](#)[Full Screen / Esc](#)[Printer-friendly Version](#)[Interactive Discussion](#)

contribute 35.9, 19.8, 18.1, 6.4, and 19.8 %, respectively, to PM_{2.5} mass concentration at the surface layer. The contributions increase significantly in the UTLS. The largest C_{NIT} is simulated in the SASM region at 100 hPa, where NO₃⁻ accounts for 60.5 % of PM_{2.5} mass concentration. The high C_{NIT} values indicate that NO₃⁻ plays an important role in the aerosol layer in the UTLS over the TP/SASM region.

6 Mechanisms for high nitrate concentrations in the UTLS

6.1 Upward transport of nitrate from the lower troposphere

The intense convective transport of chemical species into the UTLS over the TP/SASM region during summertime has been widely discussed in previous studies (Randel et al., 2010; Bian et al., 2011a; Fadnavis et al., 2013, 2014; Qie et al., 2014; He et al., 2014). Since nitrate aerosol is simulated to be the second abundant aerosol species in the surface layer over the TP/SASM region (Fig. 7), the vertical mass transport through the deep convection in this region contributes to the accumulation of NO₃⁻ in the UTLS. Figure 11 shows the latitude–altitude cross sections of simulated concentrations of SO₄²⁻ and NO₃⁻ averaged over 70–105° E in June–August of 2005, together with the wind vectors obtained from the European Centre for Medium-Range Weather Forecasts (ECMWF) ERA-Interim Reanalysis data. High values of aerosol concentrations are found on the south slope of the Himalayas, where the deep convection exists. Although both SO₄²⁻ and NO₃⁻ are transported upward to the extratropical tropopause, the details of the vertical distributions are different. At altitudes higher than 8 km, the concentrations of NO₃⁻ do not decrease with altitude as quickly as those of SO₄²⁻, and the concentrations of NO₃⁻ over 10–40° N are higher than those of SO₄²⁻, suggesting that the different chemical mechanisms for NO₃⁻ and SO₄²⁻ have contributed to these differences in vertical distributions.

Discussion Paper	Title Page
Abstract	Introduction
Conclusions	References
Tables	Figures
◀	▶
◀	▶
Back	Close
Full Screen / Esc	
Printer-friendly Version	
Interactive Discussion	

6.2 The gas-to-aerosol conversion of HNO₃ to form nitrate

ACPD

15, 32049–32099, 2015

The gas-to-aerosol conversion of HNO₃ to form nitrate is important in nitrate budget (Liao et al., 2004; Feng and Penner, 2007) and this process is very sensitive to relative humidity (RH) and temperature (Fountoukis and Nenes, 2007; Dawson et al., 2007). High RH is favorable for NO₃⁻ formation. As the temperature falls, the gas-phase oxidation of SO₂ decreases (Yao et al., 2002; Seinfeld and Pandis, 2006; X. Y. Zhang et al., 2012), while the gas-to-aerosol partition of HNO₃ (the formation of nitrate aerosol) is promoted (Ansari and Pandis, 2000; Dawson et al., 2007). Figure 12 shows the seasonal mean horizontal distributions of RH and temperature at 100 hPa and the latitude–altitude cross sections of these two parameters averaged over 70–105° E. RH exhibits high values in the TP/SASM region, which are consistent with the high H₂O mixing ratios in this area reported in Gettelman et al. (2004), M. Park et al. (2004), and Fu et al. (2006). At 100 hPa, the locations with high RH of exceeding 45 % correspond well with those with high C_{NIT} values (Fig. 10c). The latitude–altitude cross section of RH (Fig. 13c) shows that RH has high values over the places with intense upward transport (Fig. 11). For temperature, as Fig. 12b and d shows, summertime temperatures are cold (190–200 K) at 100 hPa in the TP/SASM region, in consistent with the distribution and magnitude reported for August 2011, in He et al. (2014) on the basis of the NCEP Reanalysis data. The low temperatures over the TP/SASM region are associated with the adiabatic expansion of ascending air mass of the deep convections (Yanai et al., 1992; Park et al., 2007; He et al., 2014). Besides being the dynamic responses to enhanced convection, the low temperatures at the tropopause reinforce the upwelling activities.

Because of the favorable conditions of RH and temperature, the gas-to-aerosol conversion of HNO₃ to form nitrate can occur during the upward transport and in the UTLS. Figure 13 shows the mass budget for nitrate aerosol within the selected box of (70–105° E, 10–40° N, 8–16 km) to see the role of nitrate formation over the TP/SASM region. The horizontal mass fluxes have a net negative value of 0.10 Tg season⁻¹,

Title Page

Abstract

Introduction

Conclusions

References

Tables

Figures

◀

▶

Back

Close

Full Screen / Esc

Printer-friendly Version

Interactive Discussion



Title Page

Abstract

Introduction

Conclusions

References

Tables

Figures

◀

▶

◀
Back

▶
Close

Full Screen / Esc

Printer-friendly Version

Interactive Discussion



reducing nitrate aerosol in the selected box. The vertical transport and the gas-to-aerosol conversion of HNO_3 increase nitrate mass in the selected box, with values of 0.09 Tg season $^{-1}$ and 0.11 Tg season $^{-1}$, respectively, indicating that the gas-to-aerosol conversion plays an important role in the enhancement of nitrate in the UTLS over the TP/SASM region.

Although relatively high RH exists near the tropopause of the TP/SASM region, the air near the tropopause is still dryer compared to that in the lower altitudes. Model results show that the gas-to-aerosol partition of HNO_3 decreases with altitude over 8–16 km, indicating that the gas to aerosol conversion contributes to nitrate accumulation in the UTLS mainly during the process of upward transport. HNO_3 can be absorbed onto ice particles at low temperatures and lead to the formation of nitric acid trihydrates (NAT, $\text{HNO}_3 \cdot (\text{H}_2\text{O})_3$) in polar and tropical stratosphere (Hofmann et al., 1989; Carslaw et al., 1998; Voigt et al., 2000; Popp et al., 2006). The NAT condensation temperature is approximately 193 K (Kirner et al., 2011). As shown in Fig. 12, the temperatures around 100 hPa over the TP/SASM region are in the range of 190–200 K, which are low enough to produce some NAT particles. However, balloon-borne measurements of depolarization ratio and backscattering ratio of aerosols at Lhasa during August–October of 1999 by Kim et al. (2003) and Tobo et al. (2007) suggested that particles in the UTLS of the TP/SASM region scarcely composed of coarse and aspherical particles such as NAT.

7 Conclusions

In this work we simulate nitrate aerosol and its contribution to aerosol concentrations in the UTLS over the TP/SASM region ($70\text{--}105^\circ\text{E}$, $10\text{--}40^\circ\text{N}$) by simulation for summertime of year 2005, using the global chemical transport model GEOS-Chem driven by the assimilated meteorological fields.

Simulated HNO_3 and O_3 are evaluated to show the model's capability in simulating the $\text{NO}_x\text{-O}_3\text{-HNO}_3$ cycle over the studied region. In the UTLS, both the horizontal and

vertical distributions of simulated HNO_3 and O_3 agree well with the MLS observations. At 100 hPa, the simulated and observed HNO_3 mixing ratios averaged over the ASM/TP region are 345.9 and 301.3 pptv, respectively, and the difference lies within the confidence range of the MLS instruments. Both simulated and observed O_3 concentrations show relatively low values of less than 200 ppbv at 100 hPa over the TP/SASM region.

Averaged over the TP/SASM region, the surface-layer concentrations of SO_4^{2-} , NO_3^- , NH_4^+ , BC, and OC are simulated to be 1.69, 0.94, 0.85, 0.30, and $0.94 \mu\text{g m}^{-3}$, respectively. Nitrate is simulated to be the second largest aerosol species over the region of our interest. Comparisons of simulated aerosol concentrations with ground-based observations show that simulated summertime concentrations of SO_4^{2-} , NO_3^- , NH_4^+ , OC and BC have NMB of -15.3 , $+51.5$, $+74.9$, -57.2 and -32.2% , respectively. Note that the measurements of NO_3^- and NH_4^+ are quite limited in terms of the number of samples.

Model results show elevated concentrations of SO_4^{2-} , NO_3^- , NH_4^+ , OC, BC and $\text{PM}_{2.5}$ in the UTLS over the TP/SASM region throughout the summer. NO_3^- is simulated to be the most dominant aerosol species in the UTLS of the TP/SASM region. Accounting for NO_3^- aerosol, the GEOS-Chem model reproduces well the magnitude of aerosol extinctions above 10 km, as model results are compared with the SAGE II measurements. Simulated vertical profiles of aerosol extinction coefficients with and without nitrate aerosol show large discrepancies from 6 km to tropopause, indicating the important role of nitrate in aerosol layer in the UTLS over the TP/SASM region.

The contribution of NO_3^- to aerosols in the TP/SASM region is quantified by C_{NIT} (the ratio of nitrate concentration to $\text{PM}_{2.5}$ concentration). Over the TP/SASM region, the C_{NIT} values in summer are 5–35 % at the surface, 25–50 % at 200 hPa, and exceed 60 % at 100 hPa. The mechanisms for the accumulation of nitrate in the UTLS over the TP/SASM region include vertical transport and the gas-to-aerosol conversion of HNO_3 to form nitrate. Such gas-to-aerosol conversion occurs during the upward transport and in the UTLS. The high relative humidity and low temperature associated with the deep convections over the TP/SASM region are favorable for nitrate formation.

[Title Page](#)[Abstract](#)[Introduction](#)[Conclusions](#)[References](#)[Tables](#)[Figures](#)[◀](#)[▶](#)[◀](#)[▶](#)[Back](#)[Close](#)[Full Screen / Esc](#)[Printer-friendly Version](#)[Interactive Discussion](#)

Results from the present study indicate that nitrate is an important aerosol species in the UTLS over the ASM/TP region. Considering the scarce measurements of nitrate in the UTLS and the model uncertainties, more observational and modeling studies are needed to further explore the aerosol composition in the Asian tropopause aerosol layer.

5
**The Supplement related to this article is available online at
doi:10.5194/acpd-15-32049-2015-supplement.**

Acknowledgements. This work was supported by the National Basic Research Program of China (973 program, Grant No. 2014CB441202) and the Strategic Priority Research Program 10 of the Chinese Academy of Sciences (Grant No. XDA05100503). We gratefully acknowledge NASA, USA, for providing the MLS and SAGE II data on their website. Special thanks to Jianchun Bian for providing the ozone sonde profile data in Kunming and Lhasa.

References

- Adhikary, B., Carmichael, G. R., Tang, Y., Leung, L. R., Qian, Y., Schauer, J. J., Stone, E. A., 15 Ramanathan, V., and Ramana, M. V.: Characterization of the seasonal cycle of south Asian aerosols: a regional-scale modeling analysis, *J. Geophys. Res.*, 112, D22S22, doi:10.1029/2006JD008143, 2007.
- Alexander, B., Park, R. J., Jacob, D. J., Li, Q., Yantosca, R. M., Savarino, J., Lee, C., and Thiemens, M.: Sulfate formation in sea-salt aerosols: constraints from oxygen isotopes, *J. Geophys. Res.*, 110, D10307, doi:10.1029/2004JD005659, 2005.
- Ansari, A. S. and Pandis, S. N.: The effect of metastable equilibrium states on the partitioning 20 of nitrate between the gas and aerosol phases, *Atmos. Environ.*, 34, 157–168, 2000.
- Arimoto, R., Duce, R., Savoie, D., Prospero, J., Talbot, R., Cullen, J., Tomza, U., Lewis, N., and Ray, B.: Relationships among aerosol constituents from Asia and the North Pacific during 25 PEM-West A, *J. Geophys. Res.*, 101, 2011–2023, 1996.

[Title Page](#)[Abstract](#)[Introduction](#)[Conclusions](#)[References](#)[Tables](#)[Figures](#)[◀](#)[▶](#)[◀](#)[▶](#)[Back](#)[Close](#)[Full Screen / Esc](#)[Printer-friendly Version](#)[Interactive Discussion](#)

- Babu, S. S. and Moorthy, K. K.: Aerosol black carbon over a tropical coastal station in India, *Geophys. Res. Lett.*, 29, 2098, doi:10.1029/2002GL015662, 2002.
- Bano, T., Singh, S., Gupta, N., Soni, K., Tanwar, R., Nath, S., Arya, B., and Gera, B.: Variation in aerosol black carbon concentration and its emission estimates at the mega-city Delhi, *Int. J. Remote Sens.*, 32, 6749–6764, 2011.
- 5 Bian, J., Yan, R., and Chen, H.: Tropospheric pollutant transport to the stratosphere by Asian summer monsoon, *Chinese J. Atmos. Sci.*, 35, 897–902, 2011a.
- Bian, J., Yan, R., Chen, H., Lü, D., and Massie, S. T.: Formation of the summertime ozone 10 valley over the Tibetan Plateau: the Asian summer monsoon and air column variations, *Adv. Atmos. Sci.*, 28, 1318–1325, 2011b.
- Bian, J., Pan, L. L., Paulik, L., Vömel, H., Chen, H., and Lü, D.: In situ water vapor and ozone measurements in Lhasa and Kunming during the Asian summer monsoon, *Geophys. Res. Lett.*, 39, L19808, doi:10.1029/2012GL052996, 2012.
- Bourgeois, Q., Bey, I., and Stier, P.: A permanent aerosol layer at the tropical tropopause layer 15 driven by the intertropical convergence zone, *Atmos. Chem. Phys. Discuss.*, 12, 2863–2889, doi:10.5194/acpd-12-2863-2012, 2012.
- Bouwman, A., Lee, D., Asman, W., Dentener, F., Van Der Hoek, K., and Olivier, J.: A global high-resolution emission inventory for ammonia, *Global Biogeochem. Cy.*, 11, 561–587, 1997.
- Brewer, A. W.: Evidence for a world circulation provided by the measurements of helium and 20 water vapour distribution in the stratosphere, *Q. J. Roy. Meteor. Soc.*, 75, 351–363, 1949.
- Carrico, C. M., Bergin, M. H., Shrestha, A. B., Dibb, J. E., Gomes, L., and Harris, J. M.: The importance of carbon and mineral dust to seasonal aerosol properties in the Nepal Himalaya, *Atmos. Environ.*, 37, 2811–2824, 2003.
- Carlsaw, K., Wirth, M., Tsias, A., Luo, B., Dörnbrack, A., Leutbecher, M., Volkert, H., Renger, W., 25 Bacmeister, J., and Peter, T.: Particle microphysics and chemistry in remotely observed mountain polar stratospheric clouds, *J. Geophys. Res.*, 103, 5785–5796, 1998.
- Chatterjee, A., Adak, A., Singh, A. K., Srivastava, M. K., Ghosh, S. K., Tiwari, S., Devara, P. C., and Raha, S.: Aerosol chemistry over a high altitude station at northeastern Himalayas, India, *PLoS one*, 5, e11122, doi:10.1371/journal.pone.0011122, 2010.
- 30 Chatterjee, A., Ghosh, S. K., Adak, A., Singh, A. K., Devara, P. C., and Raha, S.: Effect of dust and anthropogenic aerosols on columnar aerosol optical properties over Darjeeling (2200 m.a.s.l.), Eastern Himalayas, India, *PLoS one*, 7, e40286, doi:10.1371/journal.pone.0040286, 2012.

[Title Page](#)[Abstract](#)[Introduction](#)[Conclusions](#)[References](#)[Tables](#)[Figures](#)[◀](#)[▶](#)[◀](#)[▶](#)[Back](#)[Close](#)[Full Screen / Esc](#)[Printer-friendly Version](#)[Interactive Discussion](#)

- Chen, H., Bian, J., and Lü, D.: Advances and prospects in the study of stratosphere–troposphere exchange, Chinese J. Atmos. Sci., 30, 813–820, doi:10.1006-9895(2006)30:5<813:SDLCXP>2.0.TX;2-A, 2006.
- 5 Chowdhury, Z., Zheng, M., Schauer, J. J., Sheesley, R. J., Salmon, L. G., Cass, G. R., and Russell, A. G.: Speciation of ambient fine organic carbon particles and source apportionment of $\text{PM}_{2.5}$ in Indian cities, J. Geophys. Res., 112, D15303, doi:10.1029/2007JD008386, 2007.
- Chu, W., McCormick, M., Lenoble, J., Brogniez, C., and Pruvost, P.: SAGE II inversion algorithm, J. Geophys. Res., 94, 8339–8351, 1989.
- 10 Collins, W. J., Stevenson, D. S., Johnson, C. E., and Derwent, R. G.: The European regional ozone distribution and its links with the global scale for the years 1992 and 2015, Atmos. Environ., 34, 255–267, 2000.
- Considine, D. B., Rosenfield, J. E., and Fleming, E. L.: An interactive model study of the influence of the Mount Pinatubo aerosol on stratospheric methane and water trends, J. Geophys. Res., 106, 27711–27727, doi:10.1029/2001jd000331, 2001.
- 15 Considine, D. B., Logan, J. A., and Olsen, M. A.: Evaluation of near-tropopause ozone distributions in the Global Modeling Initiative combined stratosphere/troposphere model with ozonesonde data, Atmos. Chem. Phys., 8, 2365–2385, doi:10.5194/acp-8-2365-2008, 2008.
- Datta, A., Sharma, S., Harit, R., Kumar, V., Mandal, T., and Pathak, H.: Ammonia emission from subtropical crop land area in India, Asia-Pac. J. Atmos. Sci., 48, 275–281, 2012.
- 20 Dawson, J. P., Adams, P. J., and Pandis, S. N.: Sensitivity of $\text{PM}_{2.5}$ to climate in the Eastern US: a modeling case study, Atmos. Chem. Phys., 7, 4295–4309, doi:10.5194/acp-7-4295-2007, 2007.
- Decesari, S., Facchini, M. C., Carbone, C., Giulianelli, L., Rinaldi, M., Finessi, E., Fuzzi, S., Marignoni, A., Cristofanelli, P., Duchi, R., Bonasoni, P., Vuillermoz, E., Cozic, J., Jaffrezo, J. L., and Laj, P.: Chemical composition of PM_{10} and PM_1 at the high-altitude Himalayan station Nepal Climate Observatory-Pyramid (NCO-P) (5079 m a.s.l.), Atmos. Chem. Phys., 10, 4583–4596, doi:10.5194/acp-10-4583-2010, 2010.
- 25 Dobson, G. M. B.: Origin and distribution of the polyatomic molecules in the atmosphere, P. Roy. Soc. A.-Math. Phy., 236, 187–193, 1956.
- Drury, E., Jacob, D. J., Spurr, R. J., Wang, J., Shinozuka, Y., Anderson, B. E., Clarke, A. D., Dibb, J., McNaughton, C., and Weber, R.: Synthesis of satellite (MODIS), aircraft (ICARTT), and surface (IMPROVE, EPA–AQS, AERONET) aerosol observations over eastern North

[Title Page](#)[Abstract](#)[Introduction](#)[Conclusions](#)[References](#)[Tables](#)[Figures](#)[◀](#)[▶](#)[◀](#)[▶](#)[Back](#)[Close](#)[Full Screen / Esc](#)[Printer-friendly Version](#)[Interactive Discussion](#)

Summertime nitrate in the upper troposphere and lower stratosphere

Y. Gu and H. Liao

[Title Page](#)

[Abstract](#)

[Introduction](#)

[Conclusions](#)

[References](#)

[Tables](#)

[Figures](#)

◀

▶

[Back](#)

[Close](#)

[Full Screen / Esc](#)

[Printer-friendly Version](#)

[Interactive Discussion](#)



- America to improve MODIS aerosol retrievals and constrain surface aerosol concentrations and sources, *J. Geophys. Res.*, 115, D14204, doi:10.1029/2009JD012629, 2010.
- Duncan, B. N., Strahan, S. E., Yoshida, Y., Steenrod, S. D., and Livesey, N.: Model study of the cross-tropopause transport of biomass burning pollution, *Atmos. Chem. Phys.*, 7, 3713–3736, doi:10.5194/acp-7-3713-2007, 2007.
- Dutkiewicz, V. A., Alvi, S., Gauri, B. M., Choudhary, M. I., and Husain, L.: Black carbon aerosols in urban air in South Asia, *Atmos. Environ.*, 43, 1737–1744, 2009.
- Evans, M. and Jacob, D. J.: Impact of new laboratory studies of N_2O_5 hydrolysis on global model budgets of tropospheric nitrogen oxides, ozone, and OH, *Geophys. Res. Lett.*, 32, L09813, doi:10.1029/2005GL022469, 2005.
- Fadnavis, S., Semeniuk, K., Pozzoli, L., Schultz, M. G., Ghude, S. D., Das, S., and Kakatkar, R.: Transport of aerosols into the UTLS and their impact on the Asian monsoon region as seen in a global model simulation, *Atmos. Chem. Phys.*, 13, 8771–8786, doi:10.5194/acp-13-8771-2013, 2013.
- Fadnavis, S., Semeniuk, K., Schultz, M. G., Mahajan, A., Pozzoli, L., Sonbawane, S., and Kiefer, M.: Transport pathways of peroxyacetyl nitrate in the upper troposphere and lower stratosphere from different monsoon systems during the summer monsoon season, *Atmos. Chem. Phys. Discuss.*, 14, 20159–20195, doi:10.5194/acpd-14-20159-2014, 2014.
- Fairlie, T. D., Jacob, D. J., and Park, R. J.: The impact of transpacific transport of mineral dust in the United States, *Atmos. Environ.*, 41, 1251–1266, 2007.
- Feng, Y. and Penner, J. E.: Global modeling of nitrate and ammonium: Interaction of aerosols and tropospheric chemistry, *J. Geophys. Res.*, 112, D01304, doi:10.1029/2005JD006404, 2007.
- Fisher, J. A., Jacob, D. J., Wang, Q., Bahreini, R., Carouge, C. C., Cubison, M. J., Dibb, J. E., Diehl, T., Jimenez, J. L., and Leibensperger, E. M.: Sources, distribution, and acidity of sulfate–ammonium aerosol in the Arctic in winter–spring, *Atmos. Environ.*, 45, 7301–7318, 2011.
- Fountoukis, C. and Nenes, A.: ISORROPIA II: a computationally efficient thermodynamic equilibrium model for $\text{K}^+–\text{Ca}^{2+}–\text{Mg}^{2+}–\text{NH}_4^+–\text{Na}^+–\text{SO}_4^{2-}–\text{NO}_3^-–\text{Cl}^-–\text{H}_2\text{O}$ aerosols, *Atmos. Chem. Phys.*, 7, 4639–4659, doi:10.5194/acp-7-4639-2007, 2007.
- Froyd, K. D., Murphy, D. M., Sanford, T. J., Thomson, D. S., Wilson, J. C., Pfister, L., and Lait, L.: Aerosol composition of the tropical upper troposphere, *Atmos. Chem. Phys.*, 9, 4363–4385, doi:10.5194/acp-9-4363-2009, 2009.

Summertime nitrate in the upper troposphere and lower stratosphere

Y. Gu and H. Liao

- Fu, R., Hu, Y., Wright, J. S., Jiang, J. H., Dickinson, R. E., Chen, M., Filipiak, M., Read, W. G., Waters, J. W., and Wu, D. L.: Short circuit of water vapor and polluted air to the global stratosphere by convective transport over the Tibetan Plateau, *P. Natl. Acad. Sci. USA*, 103, 5664–5669, 2006.
- Fu, T.-M., Cao, J. J., Zhang, X. Y., Lee, S. C., Zhang, Q., Han, Y. M., Qu, W. J., Han, Z., Zhang, R., Wang, Y. X., Chen, D., and Henze, D. K.: Carbonaceous aerosols in China: top-down constraints on primary sources and estimation of secondary contribution, *Atmos. Chem. Phys.*, 12, 2725–2746, doi:10.5194/acp-12-2725-2012, 2012.
- Ganguly, D., Jayaraman, A., and Gadhavi, H.: Physical and optical properties of aerosols over an urban location in western India: seasonal variabilities, *J. Geophys. Res.*, 111, D24206, doi:10.1029/2006JD007392, 2006.
- George, S. K. and Nair, P. R.: Aerosol mass loading over the marine environment of Arabian Sea during ICARB: sea-salt and non-sea-salt components, *J. Earth Syst. Sci.*, 117, 333–344, 2008.
- George, S. K., Nair, P. R., Parameswaran, K., Jacob, S., and Abraham, A.: Seasonal trends in chemical composition of aerosols at a tropical coastal site of India, *J. Geophys. Res.*, 113, D16209, doi:10.1029/2007JD009507, 2008.
- Gettelman, A., Kinnison, D. E., Dunkerton, T. J., and Brasseur, G. P.: Impact of monsoon circulations on the upper troposphere and lower stratosphere, *J. Geophys. Res.*, 109, D22101, doi:10.1029/2004JD004878, 2004.
- Guenther, A., Karl, T., Harley, P., Wiedinmyer, C., Palmer, P. I., and Geron, C.: Estimates of global terrestrial isoprene emissions using MEGAN (Model of Emissions of Gases and Aerosols from Nature), *Atmos. Chem. Phys. Discuss.*, 6, 107–173, doi:10.5194/acpd-6-107-2006, 2006.
- Hack, J. J.: Parameterization of moist convection in the National Center for Atmospheric Research community climate model (CCM2), *J. Geophys. Res.*, 99, 5551–5568, doi:10.1029/93jd03478, 1994.
- He, Q. S., Li, C. C., Ma, J. Z., Wang, H. Q., Yan, X. L., Liang, Z. R., and Qi, G. M.: Enhancement of aerosols in UTLS over the Tibetan Plateau induced by deep convection during the Asian summer monsoon, *Atmos. Chem. Phys. Discuss.*, 14, 3169–3191, doi:10.5194/acpd-14-3169-2014, 2014.
- Hegde, P., Sudheer, A., Sarin, M., and Manjunatha, B.: Chemical characteristics of atmospheric aerosols over southwest coast of India, *Atmos. Environ.*, 41, 7751–7766, 2007.

Discussion Paper | Discussion Paper

[Title Page](#)

[Abstract](#)

[Introduction](#)

[Conclusions](#)

[References](#)

[Tables](#)

[Figures](#)

◀

▶

◀
Back

▶
Close

[Full Screen / Esc](#)

[Printer-friendly Version](#)

[Interactive Discussion](#)



- Hofmann, D., Rosen, J., Harder, J., and Hereford, J.: Balloon-borne measurements of aerosol, condensation nuclei, and cloud particles in the stratosphere at McMurdo Station, Antarctica, during the spring of 1987, *J. Geophys. Res.*, 94, 11253–11269, doi:10.1029/JD094iD09p11253, 1989.
- Huang, C., Chen, C. H., Li, L., Cheng, Z., Wang, H. L., Huang, H. Y., Streets, D. G., Wang, Y. J., Zhang, G. F., and Chen, Y. R.: Emission inventory of anthropogenic air pollutants and VOC species in the Yangtze River Delta region, China, *Atmos. Chem. Phys.*, 11, 4105–4120, doi:10.5194/acp-11-4105-2011, 2011.
- Huang, X., Song, Y., Li, M., Li, J., Huo, Q., Cai, X., Zhu, T., Hu, M., and Zhang, H.: A high-resolution ammonia emission inventory in China, *Global Biogeochem. Cy.*, 26, GB1030, doi:10.1029/2011GB004161, 2012.
- Husain, L., Dutkiewicz, V. A., Khan, A., and Ghauri, B. M.: Characterization of carbonaceous aerosols in urban air, *Atmos. Environ.*, 41, 6872–6883, 2007.
- Jacob, D. J.: Heterogeneous chemistry and tropospheric ozone, *Atmos. Environ.*, 34, 2131–2159, 2000.
- Jaeglé, L., Quinn, P. K., Bates, T. S., Alexander, B., and Lin, J.-T.: Global distribution of sea salt aerosols: new constraints from in situ and remote sensing observations, *Atmos. Chem. Phys.*, 11, 3137–3157, doi:10.5194/acp-11-3137-2011, 2011.
- Jayaraman, A., Gadhavi, H., Ganguly, D., Misra, A., Ramachandran, S., and Rajesh, T.: Spatial variations in aerosol characteristics and regional radiative forcing over India: measurements and modeling of 2004 road campaign experiment, *Atmos. Environ.*, 40, 6504–6515, 2006.
- Jeong, J. I. and Park, R. J.: Effects of the meteorological variability on regional air quality in East Asia, *Atmos. Environ.*, 69, 46–55, 2013.
- Jiang, H., Liao, H., Pye, H. O. T., Wu, S., Mickley, L. J., Seinfeld, J. H., and Zhang, X. Y.: Projected effect of 2000–2050 changes in climate and emissions on aerosol levels in China and associated transboundary transport, *Atmos. Chem. Phys.*, 13, 7937–7960, doi:10.5194/acp-13-7937-2013, 2013.
- Kar, J., Bremer, H., Drummond, J. R., Rochon, Y. J., Jones, D., Nichitiu, F., Zou, J., Liu, J., Gille, J. C., and Edwards, D. P.: Evidence of vertical transport of carbon monoxide from measurements of pollution in the troposphere (MOPITT), *Geophys. Res. Lett.*, 31, L23105, doi:10.1029/2004GL021128, 2004.

**Summertime nitrate
in the upper
troposphere and
lower stratosphere**

Y. Gu and H. Liao

[Title Page](#)[Abstract](#)[Introduction](#)[Conclusions](#)[References](#)[Tables](#)[Figures](#)[Back](#)[Close](#)[Full Screen / Esc](#)[Printer-friendly Version](#)[Interactive Discussion](#)

- Kim, J., Song, C. H., Ghim, Y., Won, J., Yoon, S., Carmichael, G., and Woo, J. H.: An investigation on NH_3 emissions and particulate $\text{NH}_4^+ - \text{NO}_3^-$ formation in East Asia, *Atmos. Environ.*, 40, 2139–2150, 2006.
- 5 Kim, Y.-S., Shibata, T., Iwasaka, Y., Shi, G., Zhou, X., Tamura, K., and Ohashi, T.: Enhancement of aerosols near the cold tropopause in summer over Tibetan Plateau: lidar and balloonborne measurements in 1999 at Lhasa, Tibet, China, in: *Lidar Remote Sensing for Industry and Environment Monitoring III*, edited by: Singh U. N., Itabe, T., and Liu, Z., *Proceedings of SPIE*, Hangzhou, China, 4893, 496–503, 2003.
- 10 Kirner, O., Ruhnke, R., Buchholz-Dietsch, J., Jöckel, P., Brühl, C., and Steil, B.: Simulation of polar stratospheric clouds in the chemistry-climate-model EMAC via the submodel PSC, *Geosci. Model Dev.*, 4, 169–182, doi:10.5194/gmd-4-169-2011, 2011.
- Kulkarni, P. and Ramachandran, S.: Comparison of aerosol extinction between lidar and SAGE II over Gadanki, a tropical station in India, *Ann. Geophys.*, 33, 351–362, doi:10.5194/angeo-33-351-2015, 2015.
- 15 Kulshrestha, U., Saxena, A., Kumar, N., Kumari, K., and Srivastava, S.: Chemical composition and association of size-differentiated aerosols at a suburban site in a semi-arid tract of India, *J. Atmos. Chem.*, 29, 109–118, 1998.
- Latha, K. M. and Badarinath, K.: Seasonal variations of black carbon aerosols and total aerosol mass concentrations over urban environment in India, *Atmos. Environ.*, 39, 4129–4141, 20
- 20 2005.
- Lau, K. M., Kim, M. K., and Kim, K. M.: Asian summer monsoon anomalies induced by aerosol direct forcing: the role of the Tibetan Plateau, *Clim. Dynam.*, 26, 855–864, doi:10.1007/s00382-006-0114-z, 2006.
- 25 Lawrence, M. G. and Lelieveld, J.: Atmospheric pollutant outflow from southern Asia: a review, *Atmos. Chem. Phys.*, 10, 11017–11096, doi:10.5194/acp-10-11017-2010, 2010.
- Lelieveld, J., Crutzen, P. J., Ramanathan, V., Andreae, M. O., Brenninkmeijer, C. A. M., Campos, T., Cass, G. R., Dickerson, R. R., Fischer, H., de Gouw, J. A., Hansel, A., Jefferson, A., Kley, D., de Laat, A. T. J., Lal, S., Lawrence, M. G., Lobert, J. M., Mayol-Bracero, O. L., Mitra, A. P., Novakov, T., Oltmans, S. J., Prather, K. A., Reiner, T., Rodhe, H., Scheeren, H. A., Sikka, D., and Williams, J.: The Indian Ocean Experiment: widespread air pollution from South and Southeast Asia, *Science*, 291, 1031–1036, doi:10.1126/science.1057103, 2001.
- 30

[Title Page](#)[Abstract](#)[Introduction](#)[Conclusions](#)[References](#)[Tables](#)[Figures](#)[◀](#)[▶](#)[◀](#)[▶](#)[Back](#)[Close](#)[Full Screen / Esc](#)[Printer-friendly Version](#)[Interactive Discussion](#)

- Leon, J.-F., Chazette, P., Dulac, F., Pelon, J., Flamant, C., Bonazzola, M., Foret, G., Alfaro, S., Cachier, H., and Cautenet, S.: Large-scale advection of continental aerosols during IN-DOEX, *J. Geophys. Res.*, 106, 28427–28428, 2001.
- Li, Q., Jiang, J. H., Wu, D. L., Read, W. G., Livesey, N. J., Waters, J. W., Zhang, Y., Wang, B., Filippiak, M. J., and Davis, C. P.: Convective outflow of South Asian pollution: A global CTM simulation compared with EOS MLS observations, *Geophys. Res. Lett.*, 32, L14826, doi:10.1029/2005GL022762, 2005.
- Liao, H. and Seinfeld, J. H.: Global impacts of gas-phase chemistry-aerosol interactions on direct radiative forcing by anthropogenic aerosols and ozone, *J. Geophys. Res.*, 110, D18208, doi:10.1029/2005JD005907, 2005.
- Liao, H., Adams, P. J., Chung, S. H., Seinfeld, J. H., Mickley, L. J., and Jacob, D. J.: Interactions between tropospheric chemistry and aerosols in a unified general circulation model, *J. Geophys. Res.*, 108, 4001, doi:10.1029/2001JD001260, 2003.
- Liao, H., Seinfeld, J. H., Adams, P. J., and Mickley, L. J.: Global radiative forcing of coupled tropospheric ozone and aerosols in a unified general circulation model, *J. Geophys. Res.*, 109, D16207, doi:10.1029/2003JD004456, 2004.
- Liu, H., Jacob, D. J., Bey, I., and Yantosca, R. M.: Constraints from ^{210}Pb and ^{7}Be on wet deposition and transport in a global three-dimensional chemical tracer model driven by assimilated meteorological fields, *J. Geophys. Res.*, 106, 12109–12128, 2001.
- Liu, X., Penner, J. E., and Wang, M.: Influence of anthropogenic sulfate and black carbon on upper tropospheric clouds in the NCAR CAM3 model coupled to the IMPACT global aerosol model, *J. Geophys. Res.*, 114, D03204, doi:10.1029/2008JD010492, 2009.
- Livesey, N. J., Filippiak, M. J., Froidevaux, L., Read, W. G., Lambert, A., Santee, M. L., Jiang, J. H., Pumphrey, H. C., Waters, J. W., and Cofield, R. E.: Validation of Aura Microwave Limb Sounder O_3 and CO observations in the upper troposphere and lower stratosphere, *J. Geophys. Res.*, 113, D15S02, doi:10.1029/2007JD008805, 2008.
- Livesey, N. J., Read, W. G., Wagner, P. A., Froidevaux, L., Lambert, A., Manney, G. L., Milán Valle, L. F., Pumphrey, H. C., Santee, M. L., Schwartz, M. J., Wang, S., Fuller, R. A., Jarnot, R. F., Knosp, B. W., and Martinez, E.: Version 4.2x Level 2 data quality and description document, JPL D-33509 Rev. A, 2015.
- Lodhi, A., Ghauri, B., Khan, M. R., Rahman, S., and Shafique, S.: Particulate matter ($\text{PM}_{2.5}$) concentration and source apportionment in Lahore, *J. Brazil. Chem. Soc.*, 20, 1811–1820, 2009.

[Title Page](#)[Abstract](#)[Introduction](#)[Conclusions](#)[References](#)[Tables](#)[Figures](#)[◀](#)[▶](#)[◀](#)[▶](#)[Back](#)[Close](#)[Full Screen / Esc](#)[Printer-friendly Version](#)[Interactive Discussion](#)

Summertime nitrate in the upper troposphere and lower stratosphere

Y. Gu and H. Liao

[Title Page](#)

[Abstract](#)

[Introduction](#)

[Conclusions](#)

[References](#)

[Tables](#)

[Figures](#)

◀

▶

◀
Back

▶
Close

[Full Screen / Esc](#)

[Printer-friendly Version](#)

[Interactive Discussion](#)



- Nakamura, T., Matsumoto, K., and Uematsu, M.: Chemical characteristics of aerosols transported from Asia to the East China Sea: an evaluation of anthropogenic combined nitrogen deposition in autumn, *Atmos. Environ.*, 39, 1749–1758, 2005.
- Oberbeck, V. R., Livingston, J. M., Russell, P. B., Pueschel, R. F., Rosen, J. N., Osborn, M. T.,
5 Kritz, M. A., Snetsinger, K. G., and Ferry, G. V.: SAGE II aerosol validation: selected altitude measurements, including particle micromeasurements, *J. Geophys. Res.*, 94, 8367–8380, doi:10.1029/JD094iD06p08367, 1989.
- Pant, P., Hegde, P., Dumka, U., Sagar, R., Satheesh, S., Moorthy, K. K., Saha, A., and Srivastava, M.: Aerosol characteristics at a high-altitude location in central Himalayas: Optical properties and radiative forcing, *J. Geophys. Res.*, 111, D17206, doi:10.1029/2005JD006768,
10 2006.
- Park, M., Randel, W. J., Kinnison, D. E., Garcia, R. R., and Choi, W.: Seasonal variation of methane, water vapor, and nitrogen oxides near the tropopause: Satellite observations and model simulations, *J. Geophys. Res.*, 109, D03302, doi:10.1029/2003JD003706, 2004.
- Park, M., Randel, W. J., Gettelman, A., Massie, S. T., and Jiang, J. H.: Transport above the
15 Asian summer monsoon anticyclone inferred from Aura Microwave Limb Sounder tracers, *J. Geophys. Res.*, 112, D16309, doi:10.1029/2006JD008294, 2007.
- Park, M., Randel, W. J., Emmons, L. K., Bernath, P. F., Walker, K. A., and Boone, C. D.: Chemical isolation in the Asian monsoon anticyclone observed in Atmospheric Chemistry Experiment (ACE-FTS) data, *Atmos. Chem. Phys.*, 8, 757–764, doi:10.5194/acp-8-757-2008,
20 2008.
- Park, M., Randel, W. J., Emmons, L. K., and Livesey, N. J.: Transport pathways of carbon monoxide in the Asian summer monsoon diagnosed from Model of Ozone and Related Tracers (MOZART), *J. Geophys. Res.*, 114, D08303, doi:10.1029/2008JD010621, 2009.
- Park, R. J., Jacob, D. J., Chin, M., and Martin, R. V.: Sources of carbonaceous aerosols
25 over the United States and implications for natural visibility, *J. Geophys. Res.*, 108, 4355, doi:10.1029/2002JD003190, 2003.
- Park, R. J., Jacob, D. J., Field, B. D., Yantosca, R. M., and Chin, M.: Natural and transboundary pollution influences on sulfate–nitrate–ammonium aerosols in the United States: Implications for policy, *J. Geophys. Res.*, 109, D15204, doi:10.1029/2003JD004473, 2004.
- Pitari, G., Aquila, V., Kravitz, B., Robock, A., Watanabe, S., Cionni, I., Luca, N. D., Genova, G. D., Mancini, E., and Tilmes, S.: Stratospheric ozone response to sulfate geoengineer-
30

[Title Page](#)[Abstract](#)[Introduction](#)[Conclusions](#)[References](#)[Tables](#)[Figures](#)[◀](#)[▶](#)[◀](#)[▶](#)[Back](#)[Close](#)[Full Screen / Esc](#)[Printer-friendly Version](#)[Interactive Discussion](#)

ing: results from the Geoengineering Model Intercomparison Project (GeoMIP), *J. Geophys. Res.*, 119, 2629–2653, doi:10.1002/2013JD020566, 2014.

Popp, P. J., Marcy, T. P., Jensen, E. J., Kärcher, B., Fahey, D. W., Gao, R. S., Thompson, T. L., Rosenlof, K. H., Richard, E. C., Herman, R. L., Weinstock, E. M., Smith, J. B., May, R. D., Vömel, H., Wilson, J. C., Heymsfield, A. J., Mahoney, M. J., and Thompson, A. M.: The observation of nitric acid-containing particles in the tropical lower stratosphere, *Atmos. Chem. Phys.*, 6, 601–611, doi:10.5194/acp-6-601-2006, 2006.

Pye, H., Liao, H., Wu, S., Mickley, L. J., Jacob, D. J., Henze, D. K., and Seinfeld, J.: Effect of changes in climate and emissions on future sulfate–nitrate–ammonium aerosol levels in the United States, *J. Geophys. Res.*, 114, D01205, doi:10.1029/2008JD010701, 2009.

Qie, X., Wu, X., Yuan, T., Bian, J., and Lü, D.: Comprehensive pattern of deep convective systems over the Tibetan Plateau–South Asian monsoon region based on TRMM data, *J. Climate*, 27, 6612–6626, 2014.

Ram, K., Sarin, M., and Hegde, P.: Atmospheric abundances of primary and secondary carbonaceous species at two high-altitude sites in India: Sources and temporal variability, *Atmos. Environ.*, 42, 6785–6796, 2008.

Ramanathan, V., Li, F., Ramana, M., Praveen, P., Kim, D., Corrigan, C., Nguyen, H., Stone, E. A., Schauer, J. J., and Carmichael, G.: Atmospheric brown clouds: hemispherical and regional variations in long-range transport, absorption, and radiative forcing, *J. Geophys. Res.*, 112, D22S21, doi:10.1029/2006JD008124, 2007.

Randel, W. J. and Park, M.: Deep convective influence on the Asian summer monsoon anticyclone and associated tracer variability observed with Atmospheric Infrared Sounder (AIRS), *J. Geophys. Res.*, 111, D12314, doi:10.1029/2005JD006490, 2006.

Randel, W. J., Park, M., Emmons, L., Kinnison, D., Bernath, P., Walker, K. A., Boone, C., and Pumphrey, H.: Asian monsoon transport of pollution to the stratosphere, *Science*, 328, 611–613, 2010.

Rasch, P. J., Tilmes, S., Turco, R. P., Robock, A., Oman, L., Chen, C. C., Stenchikov, G. L., and Garcia, R. R.: An overview of geoengineering of climate using stratospheric sulphate aerosols, *Philos. Trans. R. Soc. A-Math. Phys. Eng. Sci.*, 366, 4007–4037, doi:10.1098/rsta.2008.0131, 2008.

Rastogi, N. and Sarin, M.: Long-term characterization of ionic species in aerosols from urban and high-altitude sites in western India: Role of mineral dust and anthropogenic sources, *Atmos. Environ.*, 39, 5541–5554, 2005.

[Title Page](#)

[Abstract](#)

[Introduction](#)

[Conclusions](#)

[References](#)

[Tables](#)

[Figures](#)

◀

▶

◀

▶

[Back](#)

[Close](#)

[Full Screen / Esc](#)

[Printer-friendly Version](#)

[Interactive Discussion](#)



Summertime nitrate in the upper troposphere and lower stratosphere

Y. Gu and H. Liao

- Rastogi, N. and Sarin, M.: Quantitative chemical composition and characteristics of aerosols over western India: one-year record of temporal variability, *Atmos. Environ.*, 43, 3481–3488, 2009.
- Rengarajan, R., Sarin, M., and Sudheer, A.: Carbonaceous and inorganic species in atmospheric aerosols during wintertime over urban and high-altitude sites in North India, *J. Geophys. Res.*, 112, D21307, doi:10.1029/2006JD008150, 2007.
- Russell, P. B. and McCormick, M. P.: SAGE II aerosol data validation and initial data use: An introduction and overview, *J. Geophys. Res.*, 94, 8335–8338, 1989.
- Safai, P., Kewat, S., Praveen, P., Rao, P., Momin, G., Ali, K., and Devara, P.: Seasonal variation of black carbon aerosols over a tropical urban city of Pune, India, *Atmos. Environ.*, 41, 2699–2709, 2007.
- Salam, A., Bauer, H., Kassin, K., Mohammad Ullah, S., and Puxbaum, H.: Aerosol chemical characteristics of a mega-city in Southeast Asia (Dhaka–Bangladesh), *Atmos. Environ.*, 37, 2517–2528, 2003.
- Santee, M., Lambert, A., Read, W., Livesey, N., Cofield, R., Cuddy, D., Daffer, W., Drouin, B., Froidevaux, L., and Fuller, R.: Validation of the Aura Microwave Limb Sounder HNO_3 measurements, *J. Geophys. Res.*, 112, D24S40, doi:10.1029/2007JD008721, 2007.
- Sauvage, B., Martin, R. V., van Donkelaar, A., Liu, X., Chance, K., Jaeglé, L., Palmer, P. I., Wu, S., and Fu, T.-M.: Remote sensed and in situ constraints on processes affecting tropical tropospheric ozone, *Atmos. Chem. Phys.*, 7, 815–838, doi:10.5194/acp-7-815-2007, 2007.
- Seinfeld, J. H. and Pandis, S. N.: Atmospheric chemistry and physics: from air pollution to climate change, *Environ. Sci. Policy*, 51, 212–214, 2006.
- Sharma, R. K., Bhattachari, B., Sapkota, B., Gewali, M., and Kjeldstad, B.: Black carbon aerosols variation in Kathmandu valley, Nepal, *Atmos. Environ.*, 63, 282–288, doi:10.1016/j.atmosenv.2012.09.023, 2012.
- Škerlak, B., Sprenger, M., and Wernli, H.: A global climatology of stratosphere–troposphere exchange using the ERA-Interim data set from 1979 to 2011, *Atmos. Chem. Phys.*, 14, 913–937, doi:10.5194/acp-14-913-2014, 2014.
- Stevenson, D. S., Dentener, F. J., Schultz, M. G., Ellingsen, K., Van Noije, T. P. C., Wild, O., Zeng, G., Amann, M., Atherton, C. S., and Bell, N.: Multimodel ensemble simulations of present-day and near-future tropospheric ozone, *J. Geophys. Res.*, 111, D08301, doi:10.1029/2005JD006338, 2006.

Discussion Paper | Discussion Paper

[Title Page](#)

[Abstract](#)

[Introduction](#)

[Conclusions](#)

[References](#)

[Tables](#)

[Figures](#)

◀

▶

◀

▶

[Back](#)

[Close](#)

[Full Screen / Esc](#)

[Printer-friendly Version](#)

[Interactive Discussion](#)



- Streets, D. G., Bond, T. C., Carmichael, G. R., Fernandes, S. D., Fu, Q., He, D., Klimont, Z., Nelson, S. M., Tsai, N. Y., and Wang, M. Q.: An inventory of gaseous and primary aerosol emissions in Asia in the year 2000, *J. Geophys. Res.*, 108, 30–31, 2003.
- 5 Su, H., Jiang, J. H., Lu, X. H., Penner, J. E., Read, W. G., Massie, S., Schoeberl, M. R., Co-larco, P., Livesey, N. J., and Santee, M. L.: Observed increase of TTL temperature and water vapor in polluted clouds over Asia, *J. Climate*, 24, 2728–2736, doi:10.1175/2010jcli3749.1, 2011.
- Sudheer, A. and Sarin, M.: Carbonaceous aerosols in MABL of bay of Bengal: influence of continental outflow, *Atmos. Environ.*, 42, 4089–4100, 2008.
- 10 Talukdar, R. K., Burkholder, J. B., Roberts, J. M., Portmann, R. W., and Ravishankara, A.: Heterogeneous interaction of N_2O_5 with HCl doped H_2SO_4 under stratospheric conditions: $ClNO_2$ and Cl_2 yields, *J. Phys. Chem. A*, 116, 6003–6014, 2012.
- Tang, M. J., Telford, P. J., Pope, F. D., Rkiouak, L., Abraham, N. L., Archibald, A. T., Braesicke, P., Pyle, J. A., McGregor, J., Watson, I. M., Cox, R. A., and Kalberer, M.: Heterogeneous reaction of N_2O_5 with airborne TiO_2 particles and its implication for stratospheric particle injection, *Atmos. Chem. Phys.*, 14, 6035–6048, doi:10.5194/acp-14-6035-2014, 2014.
- 15 Tare, V., Tripathi, S., Chinnam, N., Srivastava, A., Dey, S., Manar, M., Kanawade, V. P., Agarwal, A., Kishore, S., and Lal, R.: Measurements of atmospheric parameters during Indian Space Research Organization Geosphere Biosphere Program Land Campaign II at a typical location in the Ganga Basin: 2. chemical properties, *J. Geophys. Res.*, 111, D23210, doi:10.1029/2006JD007279, 2006.
- Thornton, J. A., Jaeglé, L., and McNeill, V. F.: Assessing known pathways for HO_2 loss in aqueous atmospheric aerosols: Regional and global impacts on tropospheric oxidants, *J. Geophys. Res.*, 113, D05303, doi:10.1029/2007JD009236, 2008.
- 20 Tobo, Y., Zhang, D., Iwasaka, Y., and Shi, G.: On the mixture of aerosols and ice clouds over the Tibetan Plateau: results of a balloon flight in the summer of 1999, *Geophys. Res. Lett.*, 34, L23801, doi:10.1029/2007GL031132, 2007.
- Tripathi, S., Dey, S., Tare, V., and Satheesh, S.: Aerosol black carbon radiative forcing at an industrial city in northern India, *Geophys. Res. Lett.*, 32, L08802, doi:10.1029/2005GL022515, 2005.
- 30 van der Werf, G. R., Randerson, J. T., Giglio, L., Collatz, G. J., Mu, M., Kasibhatla, P. S., Morton, D. C., DeFries, R. S., Jin, Y., and van Leeuwen, T. T.: Global fire emissions and the

[Title Page](#)[Abstract](#)[Introduction](#)[Conclusions](#)[References](#)[Tables](#)[Figures](#)[◀](#)[▶](#)[◀](#)[▶](#)[Back](#)[Close](#)[Full Screen / Esc](#)[Printer-friendly Version](#)[Interactive Discussion](#)

- contribution of deforestation, savanna, forest, agricultural, and peat fires (1997–2009), *Atmos. Chem. Phys.*, 10, 11707–11735, doi:10.5194/acp-10-11707-2010, 2010.
- Vanhellemont, F., Tetard, C., Bourassa, A., Fromm, M., Dodion, J., Fussen, D., Brogniez, C., Degegenstein, D., Gilbert, K. L., Turnbull, D. N., Bernath, P., Boone, C., and Walker, K. A.: Aerosol extinction profiles at 525 nm and 1020 nm derived from ACE imager data: comparisons with GOMOS, SAGE II, SAGE III, POAM III, and OSIRIS, *Atmos. Chem. Phys.*, 8, 2027–2037, doi:10.5194/acp-8-2027-2008, 2008.
- Venkataraman, C., Reddy, C. K., Josson, S., and Reddy, M. S.: Aerosol size and chemical characteristics at Mumbai, India, during the INDOEX-IPF (1999), *Atmos. Environ.*, 36, 1979–1991, 2002.
- Verma, S., Boucher, O., Shekar Reddy, M., Upadhyaya, H. C., Le Van, P., Binkowski, F. S., and Sharma, O. P.: Tropospheric distribution of sulphate aerosols mass and number concentration during INDOEX-IPF and its transport over the Indian Ocean: a GCM study, *Atmos. Chem. Phys.*, 12, 6185–6196, doi:10.5194/acp-12-6185-2012, 2012.
- Vernier, J.-P., Pommereau, J.-P., Garnier, A., Pelon, J., Larsen, N., Nielsen, J., Christensen, T., Cairo, F., Thomason, L., and Leblanc, T.: Tropical stratospheric aerosol layer from CALIPSO lidar observations, *J. Geophys. Res.*, 114, D00H10, doi:10.1029/2009JD011946, 2009.
- Vernier, J. P., Thomason, L., and Kar, J.: CALIPSO detection of an Asian tropopause aerosol layer, *Geophys. Res. Lett.*, 38, L07804, doi:10.1029/2010GL046614, 2011.
- Voigt, C., Schreiner, J., Kohlmann, A., Zink, P., Mauersberger, K., Larsen, N., Deshler, T., Kröger, C., Rosen, J., and Adriani, A.: Nitric acid trihydrate (NAT) in polar stratospheric clouds, *Science*, 290, 1756–1758, 2000.
- Wang, P., McCormick, M., McMaster, L., Chu, W., Swissler, T., Osborn, M., Russell, P., Oberbeck, V., Livingston, J., and Rosen, J.: SAGE II aerosol data validation based on retrieved aerosol model size distribution from SAGE II aerosol measurements, *J. Geophys. Res.*, 94, 8381–8393, doi:10.1029/JD094iD06p08381, 1989.
- Wang, Y., Logan, J. A., and Jacob, D. J.: Global simulation of tropospheric O_3 – NO_x –hydrocarbon chemistry: 2. Model evaluation and global ozone budget, *J. Geophys. Res.*, 103, 10727–10755, 1998.
- Wang, Y., Zhang, Q. Q., He, K., Zhang, Q., and Chai, L.: Sulfate-nitrate-ammonium aerosols over China: response to 2000–2015 emission changes of sulfur dioxide, nitrogen oxides, and ammonia, *Atmos. Chem. Phys.*, 13, 2635–2652, doi:10.5194/acp-13-2635-2013, 2013.

[Title Page](#)[Abstract](#)[Introduction](#)[Conclusions](#)[References](#)[Tables](#)[Figures](#)[◀](#)[▶](#)[◀](#)[▶](#)[Back](#)[Close](#)[Full Screen / Esc](#)[Printer-friendly Version](#)[Interactive Discussion](#)

- Waters, J. W., Froidevaux, L., Harwood, R. S., Jarnot, R. F., Pickett, H. M., Read, W. G., Siegel, P. H., Cofield, R. E., Filipiak, M. J., and Flower, D.: The earth observing system microwave limb sounder (EOS MLS) on the Aura satellite, *IEEE T. Geosci. Remote*, 44, 1075–1092, 2006.
- Weigel, R., Borrmann, S., Kazil, J., Minikin, A., Stohl, A., Wilson, J. C., Reeves, J. M., Kunkel, D., de Reus, M., Frey, W., Lovejoy, E. R., Volk, C. M., Viciani, S., D'Amato, F., Schiller, C., Peter, T., Schlager, H., Cairo, F., Law, K. S., Shur, G. N., Belyaev, G. V., and Curtius, J.: In situ observations of new particle formation in the tropical upper troposphere: the role of clouds and the nucleation mechanism, *Atmos. Chem. Phys.*, 11, 9983–10010, doi:10.5194/acp-11-9983-2011, 2011.
- Wesely, M.: Parameterization of surface resistances to gaseous dry deposition in regional-scale numerical models, *Atmos. Environ.*, 23, 1293–1304, 1989.
- Wu, L. T., Su, H., and Jiang, J. H.: Regional simulations of deep convection and biomass burning over South America: 2. Biomass burning aerosol effects on clouds and precipitation, *J. Geophys. Res.*, 116, D17209, doi:10.1029/2011jd016106, 2011.
- Wu, S., Mickley, L. J., Jacob, D. J., Logan, J. A., Yantosca, R. M., and Rind, D.: Why are there large differences between models in global budgets of tropospheric ozone?, *J. Geophys. Res.*, 112, D05302, doi:10.1029/2006JD007801, 2007.
- Wu, S., Mickley, L. J., Jacob, D. J., Rind, D., and Streets, D. G.: Effects of 2000–2050 changes in climate and emissions on global tropospheric ozone and the policy-relevant background surface ozone in the United States, *J. Geophys. Res.*, 113, D18312, doi:10.1029/2007JD009639, 2008.
- Xia, X., Zong, X., Cong, Z., Chen, H., Kang, S., and Wang, P.: Baseline continental aerosol over the central Tibetan plateau and a case study of aerosol transport from South Asia, *Atmos. Environ.*, 45, 7370–7378, 2011.
- Xiong, X., Houweling, S., Wei, J., Maddy, E., Sun, F., and Barnet, C.: Methane plume over south Asia during the monsoon season: satellite observation and model simulation, *Atmos. Chem. Phys.*, 9, 783–794, doi:10.5194/acp-9-783-2009, 2009.
- Yanai, M., Li, C., and Song, Z.: Seasonal heating of the Tibetan Plateau and its effects on the evolution of the Asian summer monsoon, *J. Meteorol. Soc. Jpn.*, 70, 319–351, 1992.
- Yao, X., Chan, C. K., Fang, M., Cadle, S., Chan, T., Mulawa, P., He, K., and Ye, B.: The water-soluble ionic composition of PM_{2.5} in Shanghai and Beijing, China, *Atmos. Environ.*, 36, 4223–4234, 2002.

[Title Page](#)[Abstract](#)[Introduction](#)[Conclusions](#)[References](#)[Tables](#)[Figures](#)[◀](#)[▶](#)[◀](#)[▶](#)[Back](#)[Close](#)[Full Screen / Esc](#)[Printer-friendly Version](#)[Interactive Discussion](#)

- Yin, Y., Chen, Q., Jin, L., Chen, B., Zhu, S., and Zhang, X.: The effects of deep convection on the concentration and size distribution of aerosol particles within the upper troposphere: A case study, *J. Geophys. Res.*, 117, D22202, doi:10.1029/2012JD017827, 2012.
- Zeng, G., Pyle, J. A., and Young, P. J.: Impact of climate change on tropospheric ozone and its global budgets, *Atmos. Chem. Phys.*, 8, 369–387, doi:10.5194/acp-8-369-2008, 2008.
- Zhang, G. J. and McFarlane, N. A.: Sensitivity of climate simulations to the parameterization of cumulus convection in the Canadian Climate Centre general circulation model, *Atmos. Ocean*, 33, 407–446, 1995.
- Zhang, L., Liao, H., and Li, J.: Impacts of Asian summer monsoon on seasonal and interannual variations of aerosols over eastern China, *J. Geophys. Res.*, 115, D00K05, doi:10.1029/2009JD012299, 2010.
- Zhang, N., Cao, J., Ho, K., and He, Y.: Chemical characterization of aerosol collected at Mt. Yulong in wintertime on the southeastern Tibetan Plateau, *Atmos. Res.*, 107, 76, 2012.
- Zhang, Q., Streets, D. G., Carmichael, G. R., He, K. B., Huo, H., Kannari, A., Klimont, Z., Park, I. S., Reddy, S., Fu, J. S., Chen, D., Duan, L., Lei, Y., Wang, L. T., and Yao, Z. L.: Asian emissions in 2006 for the NASA INTEX-B mission, *Atmos. Chem. Phys.*, 9, 5131–5153, doi:10.5194/acp-9-5131-2009, 2009.
- Zhang, X., Cao, J., Li, L., Arimoto, R., Cheng, Y., Huebert, B., and Wang, D.: Characterization of atmospheric aerosols over Xian in the south margin of the Loess Plateau, China, *Atmos. Environ.*, 36, 4189–4199, 2002.
- Zhang, X. Y., Wang, Y. Q., Niu, T., Zhang, X. C., Gong, S. L., Zhang, Y. M., and Sun, J. Y.: Atmospheric aerosol compositions in China: spatial/temporal variability, chemical signature, regional haze distribution and comparisons with global aerosols, *Atmos. Chem. Phys.*, 12, 779–799, doi:10.5194/acp-12-779-2012, 2012.
- Zhang, Y., Dore, A., Ma, L., Liu, X., Ma, W., Cape, J., and Zhang, F.: Agricultural ammonia emissions inventory and spatial distribution in the North China Plain, *Environ. Pollut.*, 158, 490–501, 2010.
- Zhao, X., Turco, R. P., Kao, C. Y. J., and Elliott, S.: Aerosol-induced chemical perturbations of stratospheric ozone: three-dimensional simulations and analysis of mechanisms, *J. Geophys. Res.*, 102, 3617–3637, doi:10.1029/96jd03406, 1997.

[Title Page](#)[Abstract](#)[Introduction](#)[Conclusions](#)[References](#)[Tables](#)[Figures](#)[◀](#)[▶](#)[◀](#)[▶](#)[Back](#)[Close](#)[Full Screen / Esc](#)[Printer-friendly Version](#)[Interactive Discussion](#)

Table 1. Summary of Annual Emissions of Aerosols and Aerosol Precursors in Asia (60–155° E, 10–55° N).

Species	Global	Asia
NO_x (Tg N yr $^{-1}$)		
Aircraft	0.5	0.08
Anthropogenic	28.6	9.96
Biomass burning	4.7	0.27
Fertilizer	0.7	0.31
Lightning	5.9	0.87
Soil	5.9	0.96
Total	46.3	12.45
SO_2 (Tg S yr $^{-1}$)		
Aircraft	0.1	0.01
Anthropogenic	52.6	23.46
Biomass burning	1.2	0.07
Volcanoes	4.4	1.04
No_eruption	8.9	1.78
Ship	7.4	0.94
Total	74.6	27.30
NH_3 (Tg N yr $^{-1}$)		
Anthropogenic	34.9	17.83
Natural	14.2	2.01
Biomass burning	3.5	0.21
Biofuel	1.6	0.71
Total	54.2	20.76
OC (Tg C yr $^{-1}$)		
Anthropogenic	3.1	1.42
Biomass burning	18.7	1.10
Biofuel	6.3	3.28
Biogenic	9.7	1.22
Total	37.8	7.02
BC (Tg C yr $^{-1}$)		
Anthropogenic	3.0	1.43
Biomass burning	2.2	0.12
Biofuel	1.6	0.86
Total	6.8	2.41

Summertime nitrate in the upper troposphere and lower stratosphere

Y. Gu and H. Liao

Table 2. Simulated seasonal mean concentrations of aerosols and their contributions to PM_{2.5} (in percentages in parentheses) during summertime (Jun–Aug) of 2005 for the TP/SASM, TP, and SASM regions. The unit is $\mu\text{g m}^{-3}$ for concentrations at the surface, and $10^{-2} \mu\text{g m}^{-3}$ for concentrations at 200 and 100 hPa.

	PM _{2.5}	SO ₄ ²⁻	NO ₃ ⁻	NH ₄ ⁺	OC	BC
TP/SASM						
Surface	4.73	1.70 (35.9 %)	0.94 (19.8 %)	0.85 (18.1 %)	0.94 (19.8 %)	0.30 (6.4 %)
200 hPa	16.19	3.27 (20.2 %)	7.57 (46.8 %)	2.67 (16.5 %)	2.22 (13.7 %)	0.44 (2.7 %)
100 hPa	12.14	2.60 (21.4 %)	6.90 (56.8 %)	1.43 (11.8 %)	1.05 (8.7 %)	0.16 (1.3 %)
TP						
Surface	5.79	2.16 (37.4 %)	1.17 (20.2 %)	1.13 (19.5 %)	0.99 (17.1 %)	0.34 (5.8 %)
200 hPa	19.93	4.08 (20.5 %)	9.53 (47.8 %)	3.30 (16.6 %)	2.55 (12.8 %)	0.48 (2.4 %)
100 hPa	10.87	2.60 (23.9 %)	5.72 (52.7 %)	1.38 (12.7 %)	1.02 (9.4 %)	0.15 (1.3 %)
SASM						
Surface	4.02	1.28 (31.8 %)	0.83 (20.5 %)	0.63 (15.6 %)	1.00 (24.8 %)	0.29 (7.2 %)
200 hPa	12.57	2.38 (19.0 %)	5.72 (45.5 %)	2.10 (16.7 %)	1.95 (15.5 %)	0.41 (3.3 %)
100 hPa	13.71	2.60 (19.0 %)	8.30 (60.5 %)	1.52 (11.1 %)	1.11 (8.1 %)	0.18 (1.3 %)

[Title Page](#)

[Abstract](#)

[Introduction](#)

[Conclusions](#)

[References](#)

[Tables](#)

[Figures](#)

◀

▶

◀

▶

[Back](#)

[Close](#)

[Full Screen / Esc](#)

[Printer-friendly Version](#)

[Interactive Discussion](#)



Summertime nitrate in the upper troposphere and lower stratosphere

Y. Gu and H. Liao

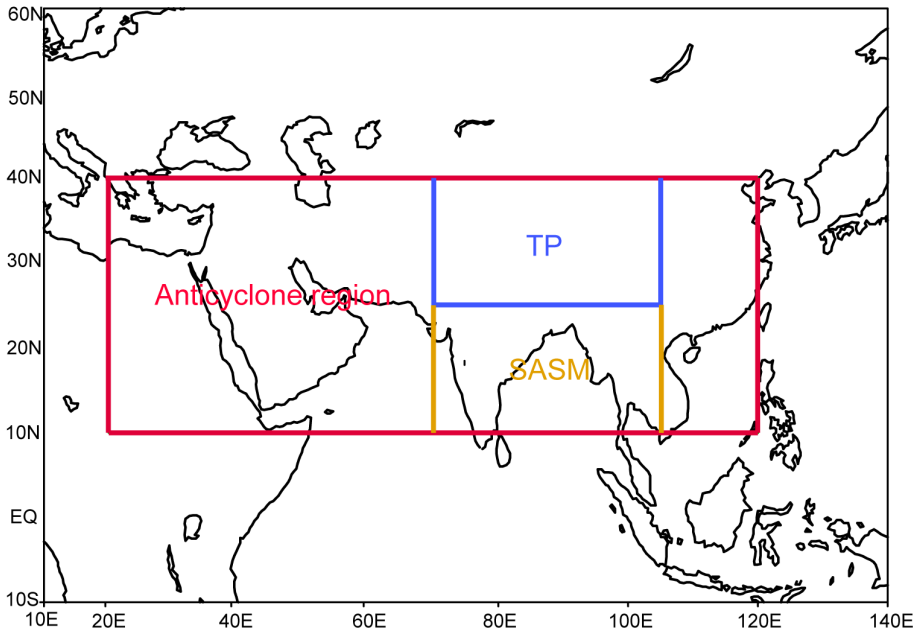


Figure 1. Regions examined in this study: the Tibetan Plateau region (TP, 70–105° E, 25–40° N), the SASM region (SASM, 70–105° E, 10–25° N), and the anticyclone region of (20–120° E, 10–40° N).

[Title Page](#)

[Abstract](#)

[Introduction](#)

[Conclusions](#)

[References](#)

[Tables](#)

[Figures](#)

[◀](#)

[▶](#)

[◀](#)

[▶](#)

[Back](#)

[Close](#)

[Full Screen / Esc](#)

[Printer-friendly Version](#)

[Interactive Discussion](#)

**Summertime nitrate
in the upper
troposphere and
lower stratosphere**

Y. Gu and H. Liao

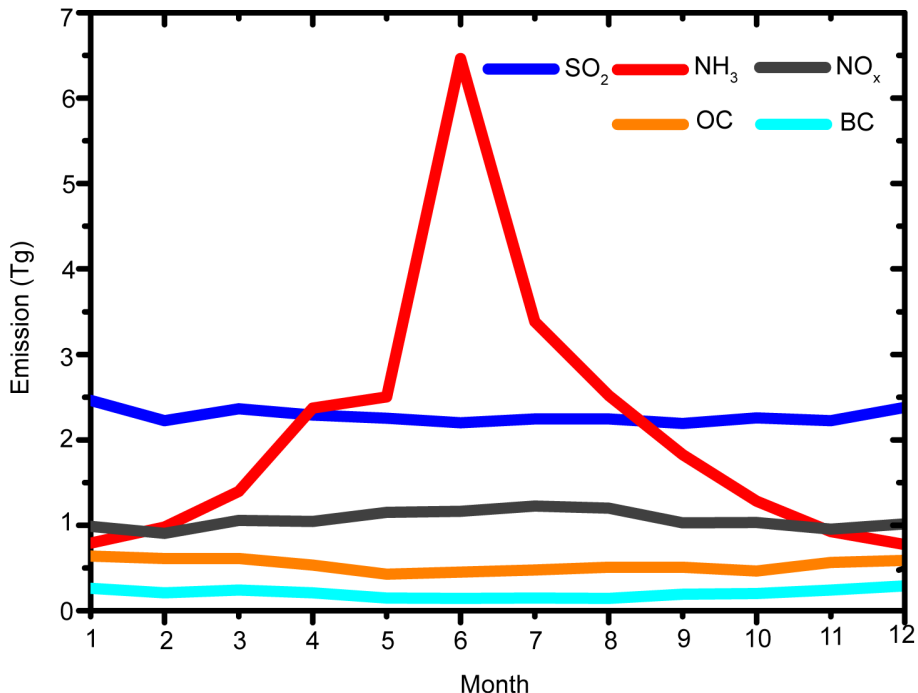


Figure 2. Monthly variations in emissions of NO_x (Tg N month⁻¹), SO₂ (Tg S month⁻¹), NH₃ (Tg N month⁻¹), OC (Tg C month⁻¹), and BC (Tg C month⁻¹) over Asia. Values shown are the total emissions (anthropogenic plus natural emissions listed in Table 1).

- [Title Page](#)
- [Abstract](#) [Introduction](#)
- [Conclusions](#) [References](#)
- [Tables](#) [Figures](#)
- [◀](#) [▶](#)
- [◀](#) [▶](#)
- [Back](#) [Close](#)
- [Full Screen / Esc](#)
- [Printer-friendly Version](#)
- [Interactive Discussion](#)

**Summertime nitrate
in the upper
troposphere and
lower stratosphere**

Y. Gu and H. Liao

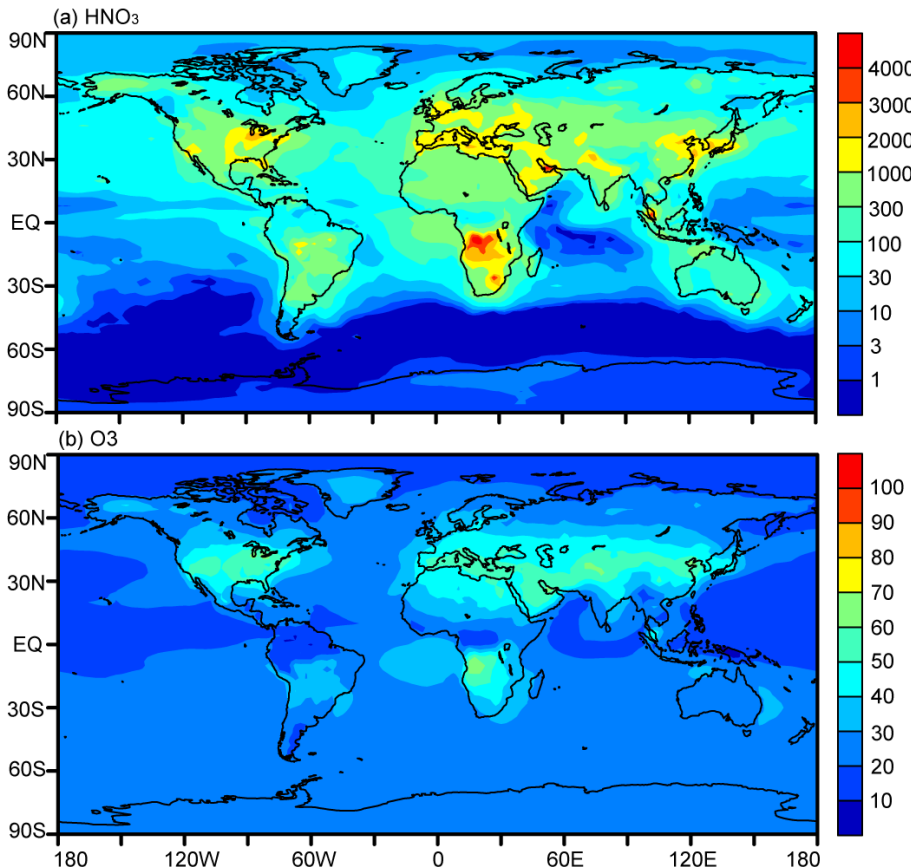


Figure 3. Simulated global distributions of surface-layer HNO_3 (pptv) and O_3 (ppbv) averaged over June–August 2005.

[Title Page](#)[Abstract](#)[Introduction](#)[Conclusions](#)[References](#)[Tables](#)[Figures](#)[Back](#)[Close](#)[Full Screen / Esc](#)[Printer-friendly Version](#)[Interactive Discussion](#)

**Summertime nitrate
in the upper
troposphere and
lower stratosphere**

Y. Gu and H. Liao

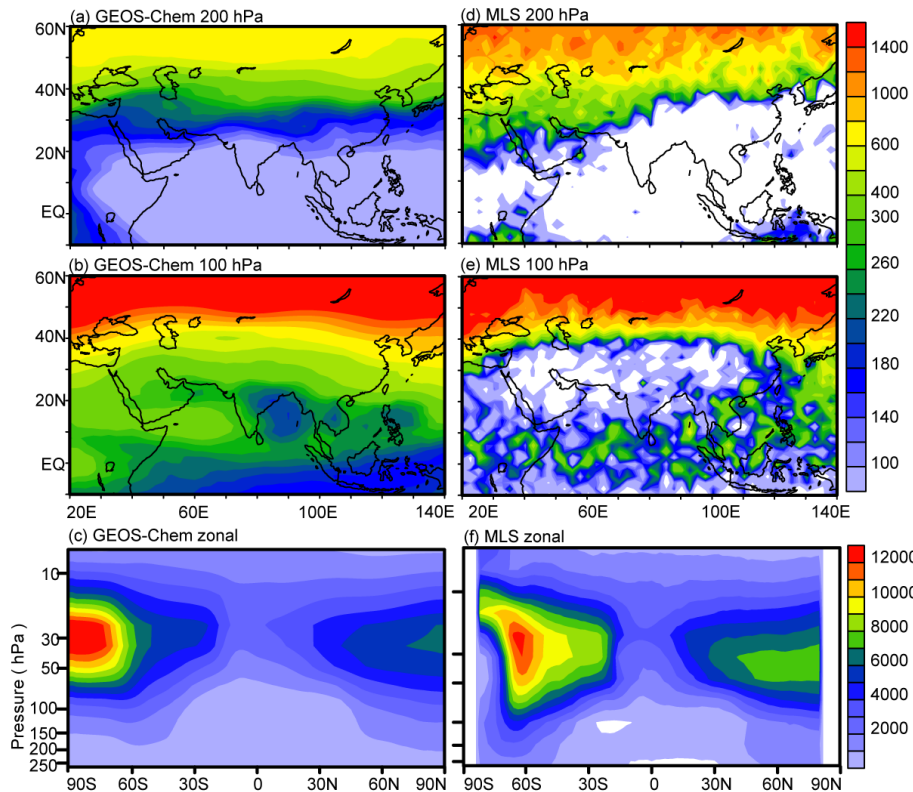


Figure 4. Comparisons of simulated HNO_3 concentrations (pptv) with observations (pptv) from MLS. (a) and (b) are simulated concentrations at 200 and 100 hPa, respectively. (c) is the latitude–altitude cross section of simulated HNO_3 concentrations averaged over 70–105° E. (d)–(f) are the same as (a)–(c), except that (d)–(f) are observations from MLS. The white areas in (d) and (f) have no datasets available from MLS. All the datasets are averaged over June–August of 2005.

[Title Page](#)[Abstract](#)[Introduction](#)[Conclusions](#)[References](#)[Tables](#)[Figures](#)[◀](#)[▶](#)[◀](#)[▶](#)[Back](#)[Close](#)[Full Screen / Esc](#)[Printer-friendly Version](#)[Interactive Discussion](#)

**Summertime nitrate
in the upper
troposphere and
lower stratosphere**

Y. Gu and H. Liao

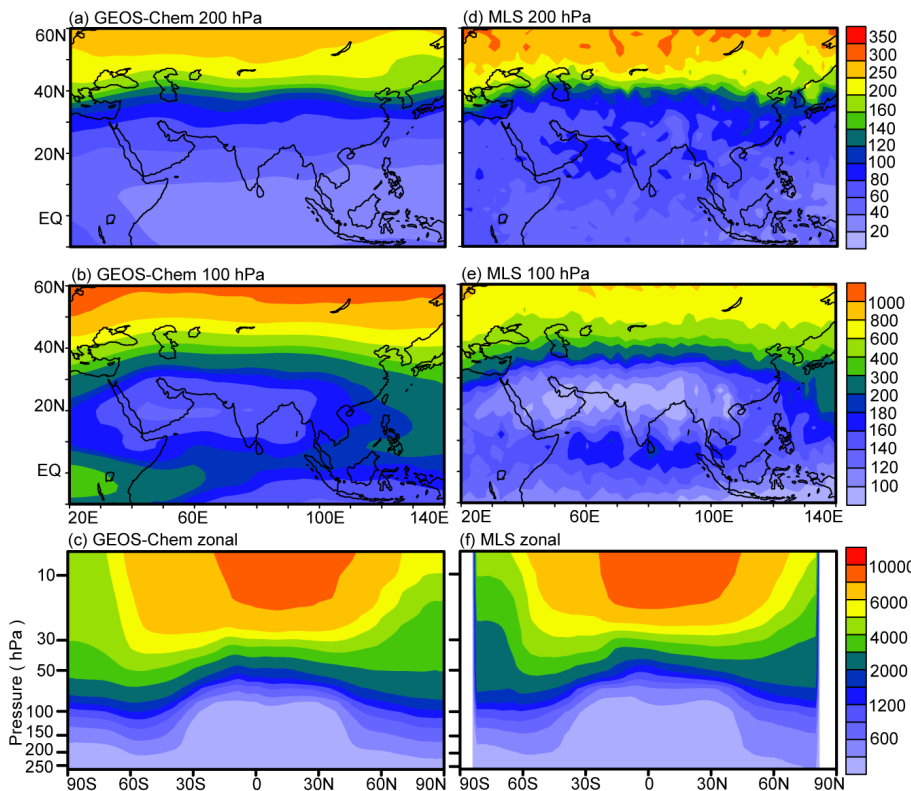


Figure 5. Comparisons of simulated O₃ concentrations (ppbv) with observations (ppbv) from MLS. **(a)** and **(b)** are simulated concentrations at 200 and 100 hPa, respectively. **(c)** is the latitude–altitude cross section of simulated O₃ concentrations averaged over 70–105° E. **(d)–(f)** are the same as **(a)–(c)**, except that **(d)–(f)** are observations from MLS. All the datasets are averaged over June–August of 2005.

[Title Page](#)[Abstract](#)[Introduction](#)[Conclusions](#)[References](#)[Tables](#)[Figures](#)[◀](#)[▶](#)[◀](#)[▶](#)[Back](#)[Close](#)[Full Screen / Esc](#)[Printer-friendly Version](#)[Interactive Discussion](#)

**Summertime nitrate
in the upper
troposphere and
lower stratosphere**

Y. Gu and H. Liao

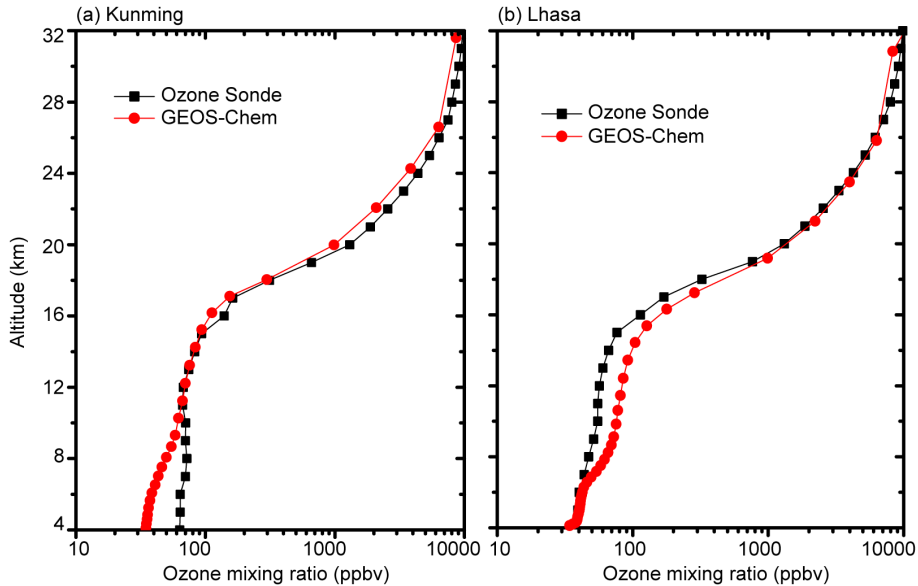


Figure 6. The simulated and observed vertical profiles of monthly mean O_3 mixing ratios at (a) Kunming and (b) Lhasa in August 2005. The measurements are shown in black, and the simulated profiles are shown in red.

[Title Page](#)[Abstract](#)[Introduction](#)[Conclusions](#)[References](#)[Tables](#)[Figures](#)[Back](#)[Close](#)[Full Screen / Esc](#)[Printer-friendly Version](#)[Interactive Discussion](#)

Summertime nitrate in the upper troposphere and lower stratosphere

Y. Gu and H. Liao

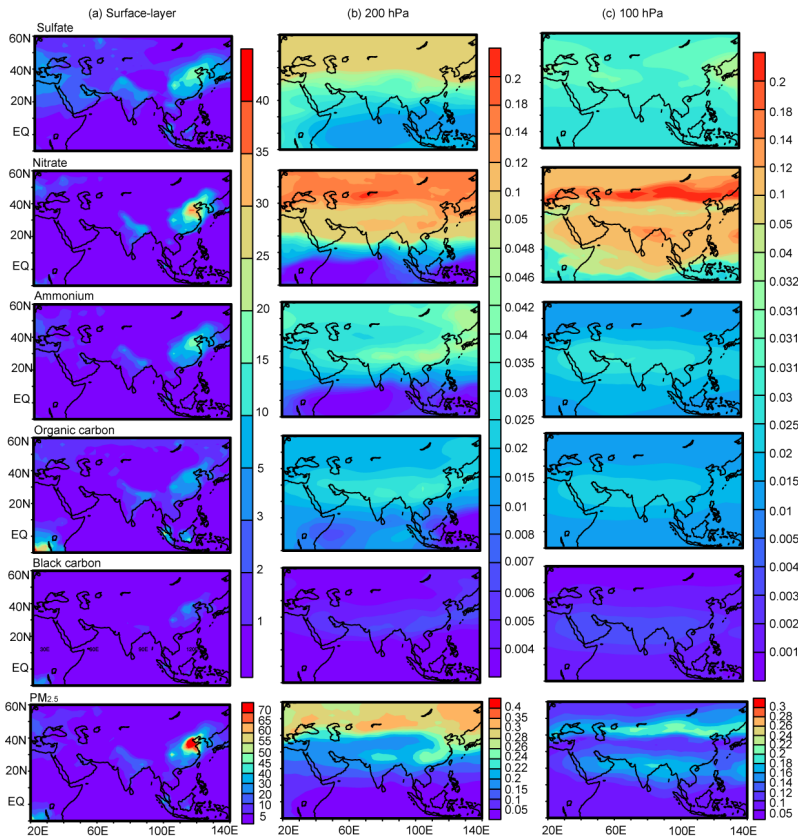


Figure 7. Simulated seasonal mean concentrations ($\mu\text{g m}^{-3}$) of sulfate, nitrate, ammonium, organic carbon, black carbon, and $\text{PM}_{2.5}$ at (a) the surface layer, (b) 200 hPa, and (c) 100 hPa, during summer (June–August) of year 2005. Note that color bars are different for concentrations at the surface, 200 hPa, and 100 hPa.

Summertime nitrate in the upper troposphere and lower stratosphere

Y. Gu and H. Liao

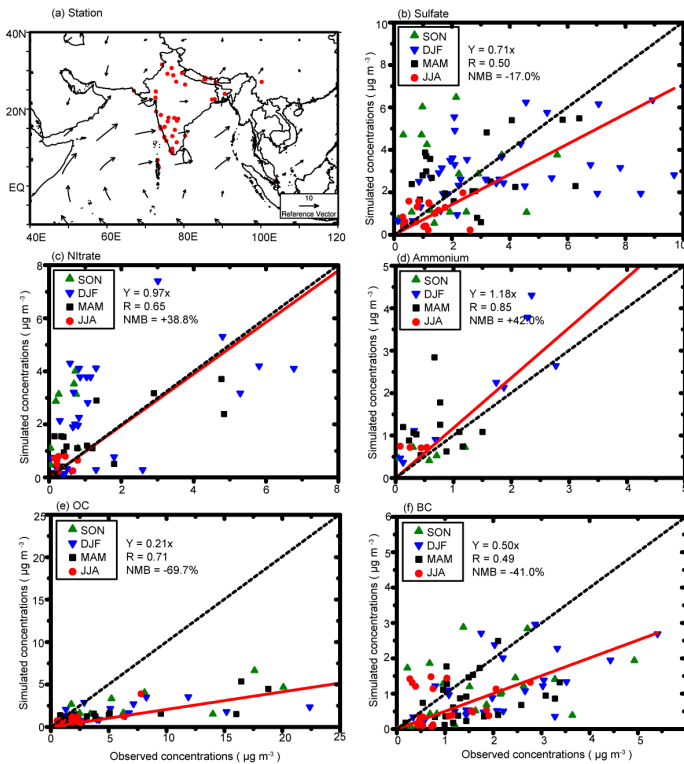


Figure 8. (a) Locations with measured aerosol concentrations from previous studies. Also shown are surface winds during summertime. (b)–(f) show the comparisons of simulated seasonal mean concentrations of sulfate, nitrate, ammonium, OC, and BC with measured values, respectively. Also shown in (b)–(f) are the 1 : 1 line (dashed), linear fit (solid line and equation), correlation coefficient between simulated and measured concentrations (R), and normalized mean bias (NMB) (defined as $NMB = \frac{\sum_{i=1}^n (P_i - O_i)}{\sum_{i=1}^n O_i} \times 100\%$, where P_i and O_i are predicted and observed concentrations at station i for each aerosol species).

Summertime nitrate in the upper troposphere and lower stratosphere

Y. Gu and H. Liao

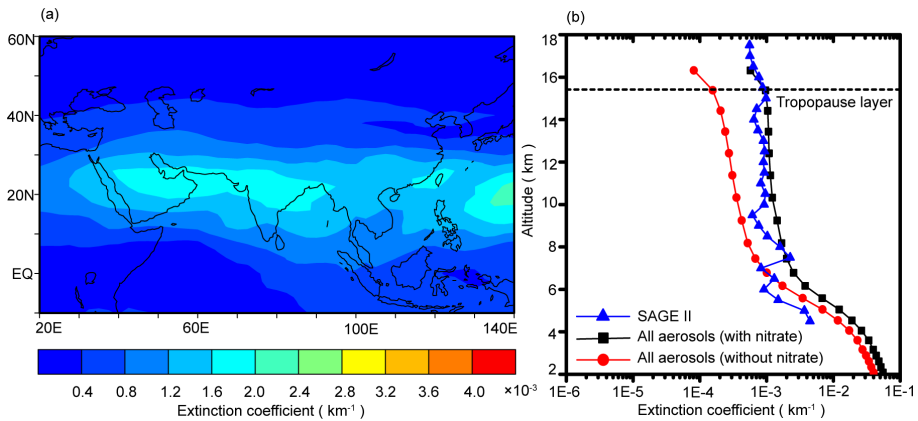


Figure 9. (a) Monthly mean distribution of aerosol extinction coefficients (km^{-1}) at 100 hPa for July of 2005. (b) Monthly mean vertical distributions of aerosol extinction coefficients (at 525 nm for SAGE II and 550 nm for GEOS-Chem) (km^{-1}) averaged over the Asian monsoon anticyclone region ($20\text{--}120^\circ\text{E}$, $10\text{--}40^\circ\text{N}$) for July of 2005. The horizontal dashed line represents the tropopause averaged over the Asian monsoon anticyclone region simulated by the GEOS-Chem model.

[Title Page](#)

[Abstract](#)

[Introduction](#)

[Conclusions](#)

[References](#)

[Tables](#)

[Figures](#)

◀

▶

◀
Back

▶
Close

[Full Screen / Esc](#)

[Printer-friendly Version](#)

[Interactive Discussion](#)

**Summertime nitrate
in the upper
troposphere and
lower stratosphere**

Y. Gu and H. Liao

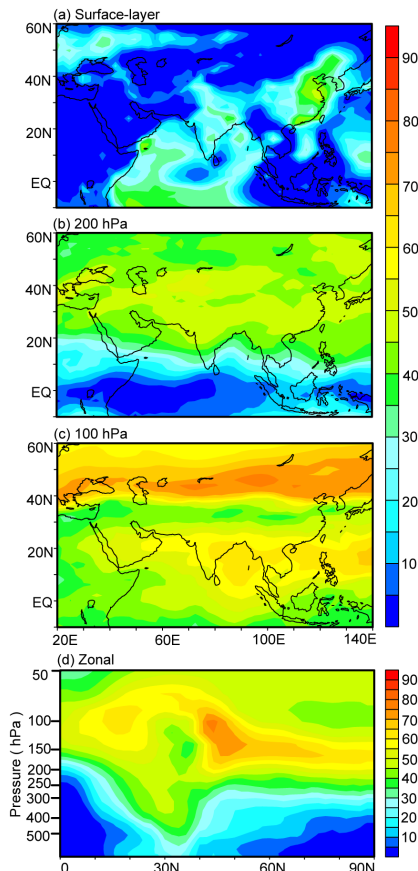


Figure 10. Simulated contributions of nitrate to PM_{2.5} ($C_{\text{NIT}} = [\text{NIT}]/[\text{PM}_{2.5}] \times 100\%$) averaged over summer (June–August) of year 2005 at (a) surface-layer, (b) 200 hPa, and (c) 100 hPa. (d) The latitude–altitude cross section of simulated C_{NIT} (%) averaged over 70–105°E.

[Title Page](#)[Abstract](#)[Introduction](#)[Conclusions](#)[References](#)[Tables](#)[Figures](#)[◀](#)[▶](#)[◀](#)[▶](#)[Back](#)[Close](#)[Full Screen / Esc](#)[Printer-friendly Version](#)[Interactive Discussion](#)

Summertime nitrate in the upper troposphere and lower stratosphere

Y. Gu and H. Liao

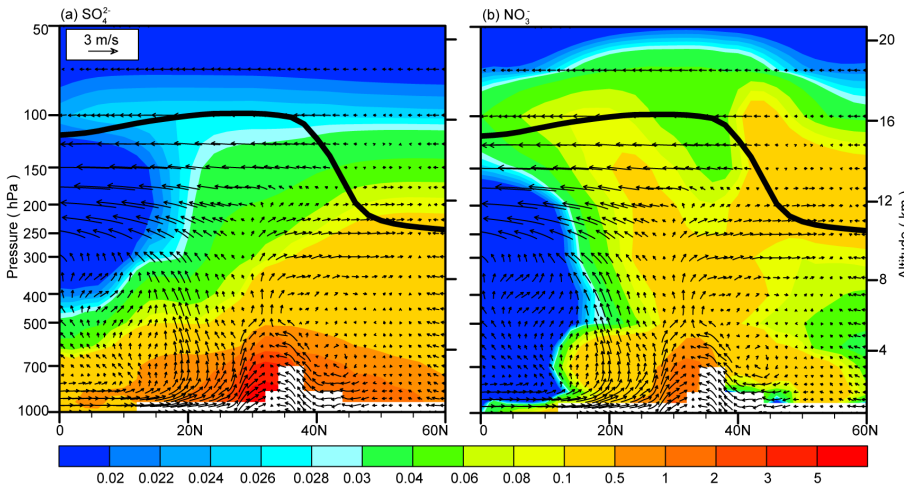


Figure 11. Latitude–altitude cross sections of simulated concentrations (color shades, $\mu\text{g m}^{-3}$) of SO_4^{2-} and NO_3^- averaged over $70\text{--}105^\circ\text{E}$ in June–August of 2005, together with the wind vectors obtained from the European Centre for Medium-Range Weather Forecasts (ECMWF) ERA-Interim Reanalysis data. The black line is the tropopause simulated by the GEOS-Chem model.

[Title Page](#)[Abstract](#)[Introduction](#)[Conclusions](#)[References](#)[Tables](#)[Figures](#)[◀](#)[▶](#)[◀](#)[▶](#)[Back](#)[Close](#)[Full Screen / Esc](#)[Printer-friendly Version](#)[Interactive Discussion](#)

Summertime nitrate in the upper troposphere and lower stratosphere

Y. Gu and H. Liao

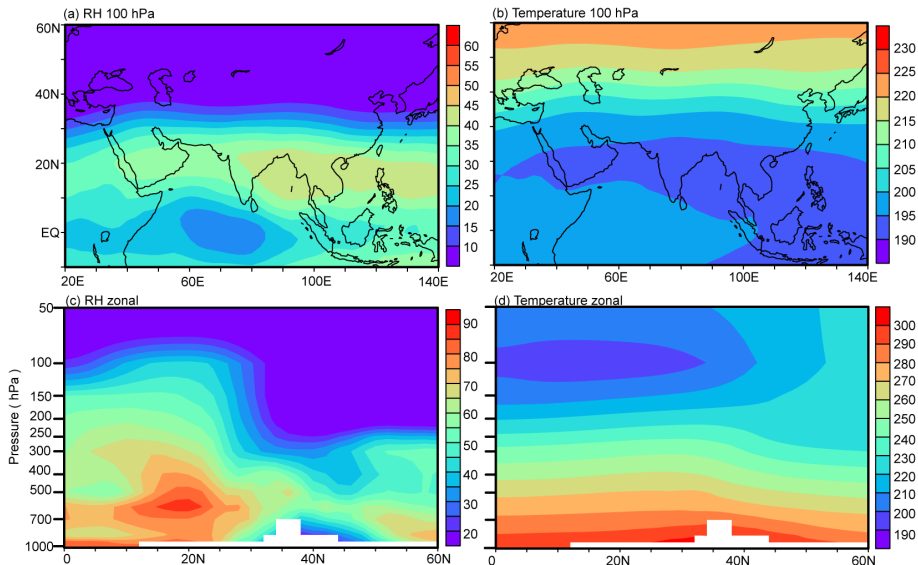


Figure 12. **(a)–(b)** Distributions of RH (%) and temperature (K) at 100 hPa. **(c)–(d)** The latitude–altitude cross sections of RH (%) and temperature (K) averaged over 70–105° E. RH and temperature are from the GEOS5 assimilated meteorological fields, and all the values are the averages over June–August of year 2005.

Title Page

Abstract

Introduction

Conclusions

References

Tables

Figures

◀

▶

◀
Back

▶
Close

Full Screen / Esc

Printer-friendly Version

Interactive Discussion

Summertime nitrate in the upper troposphere and lower stratosphere

Y. Gu and H. Liao

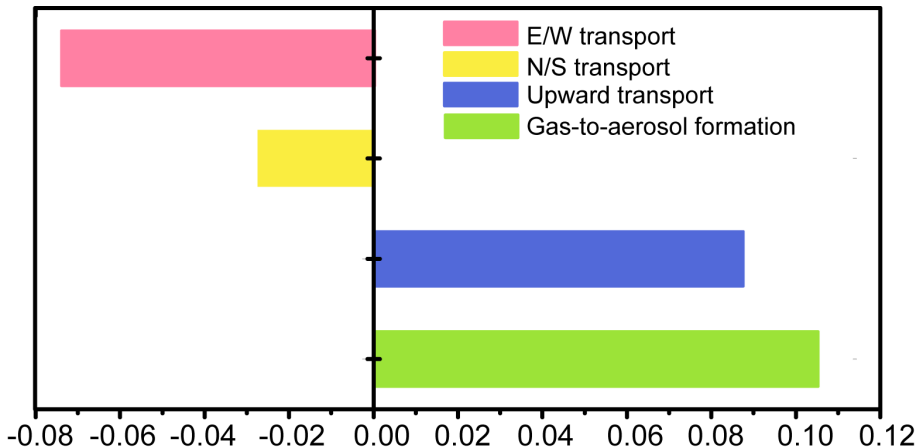


Figure 13. Mass budget for nitrate aerosol within the selected box of (70–105° E, 10–40° N, 8–16 km). E/W transport indicates net mass flux through the east and west lateral boundaries, N/S transport indicates net mass flux through the north and south lateral boundaries, and upward transport is the net mass flux through the top and bottom sides of the box. The mass flux is positive if it increases nitrate mass within the box. Unit of fluxes is Tg season⁻¹. All the values are the averages over June–August of 2005.

[Title Page](#)

[Abstract](#)

[Introduction](#)

[Conclusions](#)

[References](#)

[Tables](#)

[Figures](#)

◀

▶

[Back](#)

[Close](#)

[Full Screen / Esc](#)

[Printer-friendly Version](#)

[Interactive Discussion](#)